

Controlled fermion mixing and FCNCs in a $\Delta(27)$ 3+1 Higgs Doublet Model

A. E. Cárcamo Hernández^{a,*}, Ivo de Medeiros Varzielas^{b,†}, M.L. López-Ibáñez^{c,‡} and Aurora Melis^{d,§}

^a *Universidad Técnica Federico Santa María
and Centro Científico-Tecnológico de Valparaíso
Casilla 110-V, Valparaíso, Chile,*

^b *CFTP, Departamento de Física,
Instituto Superior Técnico,
Universidade de Lisboa,*

Avenida Rovisco Pais 1, 1049 Lisboa, Portugal

^c *CAS Key Laboratory of Theoretical Physics,
Institute of Theoretical Physics,*

Chinese Academy of Sciences, Beijing 100190, China.

^d *Laboratory of High Energy and Computational Physics,
National Institute of Chemical Physics and Biophysics,
Rāvala pst. 10, 10143 Tallinn, Estonia*

(Dated: May 20, 2021)

We propose a 3+1 Higgs Doublet Model based on the $\Delta(27)$ family symmetry supplemented by several auxiliary cyclic symmetries leading to viable Yukawa textures for the Standard Model fermions, consistent with the observed pattern of fermion masses and mixings. The charged fermion mass hierarchy and the quark mixing pattern is generated by the spontaneous breaking of the discrete symmetries due to flavons that act as Froggatt-Nielsen fields. The tiny neutrino masses arise from a radiative seesaw mechanism at one loop level, thanks to a preserved $Z_2^{(1)}$ discrete symmetry, which also leads to stable scalar and fermionic dark matter candidates. The leptonic sector features the predictive cobimaximal mixing pattern, consistent with the experimental data from neutrino oscillations. For the scenario of normal neutrino mass hierarchy, the model predicts an effective Majorana neutrino mass parameter in the range $3 \text{ meV} \lesssim m_{\beta\beta} \lesssim 18 \text{ meV}$, which is within the declared range of sensitivity of modern experiments. The model predicts Flavour Changing Neutral Currents which constrain the model, for instance, $\mu \rightarrow e$ nuclear conversion processes and Kaon mixing are found to be within the reach of the forthcoming experiments.

I. INTRODUCTION

The Standard Model (SM) is unable to describe the observed pattern of SM fermion masses and mixings, which includes the large hierarchy among its numerous Yukawa couplings. To address the flavour problem, a promising option is to add family symmetries and obtain the Yukawa couplings from an underlying theory through the spontaneous breaking of the family symmetry.

$\Delta(27)$ as a family symmetry is greatly motivated by being one of the smallest discrete groups with a triplet and anti-triplet and the interesting interplay it has with CP symmetry. $\Delta(27)$ has been used in [1–34].

We consider here a 3+1 Higgs Doublet Model (HDM) based on the $\Delta(27)$ family symmetry supplemented by several cyclic symmetries, where three of the $SU(2)$ doublets transform as an anti-triplet of $\Delta(27)$, H . The other doublet, h ,

*Electronic address: antonio.carcamo@usm.cl

†Electronic address: ivo.de@udo.edu

‡Electronic address: maloi2@uv.es

§Electronic address: aurora.melis@uv.es

does not acquire a Vacuum Expectation Value (VEV) since it is charged under a preserved $Z_2^{(1)}$ and couples only to the neutrino sector. Thus, the light active neutrino masses are generated from a radiative seesaw mechanism at one loop level mediated by the neutral components of the inert scalar doublet h and the right handed Majorana neutrinos. Due to the preserved $Z_2^{(1)}$ symmetry, our model has stable scalar and fermionic dark matter (DM) candidates. The scalar DM candidate is the lightest among the CP-even and CP-odd neutral components of the $SU(2)$ -doublet scalar h . Furthermore, the fermionic DM candidate corresponds to the lightest among the right handed Majorana neutrinos. The DM constraints can be fulfilled in our model for an appropriate region of parameter space, along similar lines of Refs. [27, 35–51]. A detailed study of the implications of DM properties in our model goes beyond the scope of this paper and is therefore deferred for a future work. The masses and mixing of the charged fermions arise from H . Realistic masses and mixing require further sources of $\Delta(27)$ breaking [8, 12, 14] (this is not specific to $\Delta(27)$, see [52]). For this purpose, the model includes flavons (singlets under the SM) that are triplets of $\Delta(27)$ and acquire VEVs at a family symmetry breaking scale, assumed to be higher than the EW breaking scale, thus allowing them to decouple from the low-energy scalar potential.

The Left-Handed (LH) leptons transform as anti-triplets of $\Delta(27)$, and the combination of charged lepton couplings to H and neutrino couplings to h leads to a model with radiative seesaw and featuring the predictive and viable cobimaximal mixing pattern, which has attracted a lot of attention and interest by the model building community due to its predictive power to yield the observed pattern of leptonic mixing [25, 30, 32, 53–62].

The quarks transform as singlets of $\Delta(27)$ but their masses still originate from Yukawa terms involving H and a dominant flavon VEV. The symmetries allow also terms with subdominant flavon VEVs which do not contribute to the masses but do produce the leading contribution to Yukawa couplings with the additional physical Higgs fields, and give rise to controlled Flavour Changing Neutral Currents (FCNCs).

Distinguishing family symmetry models that have similar predictions for the Yukawa couplings is particularly relevant, and FCNCs are arguably the most reliable way to do so (see e.g. [29, 63–65] for some recent examples). In the present model, we study the FCNCs mediated by the physical scalars in the leptonic and quark sectors in order to constrain the parameter space, and find that in particular the muon conversion process and Kaon observables already constrain this model.

The layout of this paper is as follows. In Section II we describe the proposed model and we present its symmetry and field content. Section III describes the low energy scalar potential and discusses the mass spectrum of the light scalars which play relevant roles in phenomenology. In Section IV we discuss the quark (IV A) and lepton (IV B) couplings to the scalars, showing the respective Lagrangian terms, Yukawa matrices that arise after family symmetry breaking, and model's fits to the observables. Section V analyses the constraints that arise from FCNCs in the context of this model. We conclude in Section VI.

II. THE MODEL

We consider an extension of the SM with additional family symmetry, which is broken at a high scale. The full symmetry \mathcal{G} of the model exhibits the following spontaneous symmetry breaking pattern:

$$\begin{aligned}
 \mathcal{G} &= SU(3)_C \times SU(2)_L \times U(1)_Y \times \Delta(27) \times Z_2^{(1)} \times Z_2^{(2)} \times Z_2^{(3)} \times Z_{18} \\
 &\Downarrow \Lambda \\
 &SU(3)_C \times SU(2)_L \times U(1)_Y \times Z_2^{(1)} \\
 &\Downarrow v \\
 &SU(3)_C \times U(1)_Q \times Z_2^{(1)}, \tag{1}
 \end{aligned}$$

	H	h	σ	ϕ_{123}	ϕ_1	ϕ_{23}	ϕ_3
$\Delta(27)$	$\bar{\mathbf{3}}$	$\mathbf{1}_{0,0}$	$\mathbf{1}_{0,0}$	$\mathbf{3}$	$\mathbf{3}$	$\mathbf{3}$	$\mathbf{3}$
$Z_2^{(1)}$	0	1	0	0	0	0	0
$Z_2^{(2)}$	0	0	0	0	0	1	0
$Z_2^{(3)}$	0	0	0	0	0	0	1
Z_{18}	0	0	-1	0	0	0	0

Table I: Scalar assignments under the $\Delta(27) \times Z_2^{(1)} \times Z_2^{(2)} \times Z_2^{(3)} \times Z_{18}$. Superscripts differentiate between the multiple Z_2 symmetries.

where Λ is the scale of breaking of the $\Delta(27) \times Z_2^{(1)} \times Z_2^{(2)} \times Z_2^{(3)} \times Z_{18}$ discrete group, which we assume to be much larger than the electroweak symmetry breaking scale $v = 246$ GeV. The Z_{18} symmetry and the three additional Z_2 symmetries are distinguished by superscripts and commute with $\Delta(27)$.

The model includes four scalar $SU(2)_L$ doublets, three arranged as an anti-triplet of $\Delta(27)$, H , and h which is a singlet of $\Delta(27)$, does not acquire a VEV, and is charged under the unbroken $Z_2^{(1)}$. The scalar sector is further extended, to include four flavons (SM singlets) $\Delta(27)$ triplets ϕ_A and one $\Delta(27)$ trivial singlet σ which plays the role of a Froggatt-Nielsen (FN) field. The FN field σ acquires a VEV at a very large energy scale, spontaneously breaking the Z_{18} discrete group and then giving rise to the observed SM fermion mass and mixing hierarchy. Furthermore, the $\Delta(27)$ triplet ϕ_3 is introduced to build the quark Yukawa terms invariant under the $\Delta(27)$ family symmetry. The remaining $\Delta(27)$ triplets ϕ_{123} , ϕ_{23} and ϕ_1 are introduced in order to get a light active neutrino mass matrix featuring a cobimaximal mixing pattern, thus allowing to have a very predictive lepton sector consistent with the current neutrino oscillation experimental data. The scalar assignments under the $\Delta(27) \times Z_2^{(1)} \times Z_2^{(2)} \times Z_2^{(3)} \times Z_{18}$ discrete group are shown in Table I. Here the dimensions of the $\Delta(27)$ irreducible representations are specified by the numbers in boldface and the different charges are written in additive notation.

	q_{1L}	q_{2L}	q_{3L}	u_{1R}	u_{2R}	u_{3R}	d_{1R}	d_{2R}	d_{3R}
$\Delta(27)$	$\mathbf{1}_{0,0}$	$\mathbf{1}_{0,0}$	$\mathbf{1}_{0,0}$	$\mathbf{1}_{0,0}$	$\mathbf{1}_{0,0}$	$\mathbf{1}_{0,0}$	$\mathbf{1}_{0,0}$	$\mathbf{1}_{0,0}$	$\mathbf{1}_{0,0}$
$Z_2^{(1)}$	0	0	0	0	0	0	0	0	0
$Z_2^{(2)}$	0	0	0	0	0	0	0	0	0
$Z_2^{(3)}$	0	0	0	1	1	1	1	1	1
Z_{18}	-4	-2	0	4	2	0	4	3	3

Table II: Quark assignments under the $\Delta(27) \times Z_2^{(1)} \times Z_2^{(2)} \times Z_2^{(3)} \times Z_{18}$. Superscripts differentiate between the multiple Z_2 symmetries.

	l_L	l_{1R}	l_{2R}	l_{3R}	N_{1R}	N_{2R}	N_{3R}
$\Delta(27)$	$\bar{\mathbf{3}}$	$\mathbf{1}_{0,1}$	$\mathbf{1}_{0,2}$	$\mathbf{1}_{0,1}$	$\mathbf{1}_{0,0}$	$\mathbf{1}_{0,0}$	$\mathbf{1}_{0,0}$
$Z_2^{(1)}$	0	0	0	0	1	1	1
$Z_2^{(2)}$	0	0	0	0	0	0	1
$Z_2^{(3)}$	0	0	0	0	0	0	0
Z_{18}	0	9	5	3	0	0	0

Table III: Lepton assignments under the $\Delta(27) \times Z_2^{(1)} \times Z_2^{(2)} \times Z_2^{(3)} \times Z_{18}$. Superscripts differentiate between the multiple Z_2 symmetries.

The role of the different cyclic groups is described as follows. The $Z_2^{(3)}$ symmetry is crucial for separating the $\Delta(27)$ scalar triplet ϕ_3 participating in the quark Yukawa terms from the ones appearing in the neutrino Yukawa interactions. The $Z_2^{(2)}$ symmetry is necessary for shaping a cobimaximal texture of the light neutrino mass matrix, thus allowing a reduction of the lepton sector model parameters and at the same time allowing to successfully accommodate the

neutrino oscillation experimental data. The preserved $Z_2^{(1)}$ symmetry allows the implementation of a radiative seesaw mechanism at one loop level, providing a natural explanation for the tiny masses of the light active neutrinos and also enabling stable DM candidates. Finally, the spontaneously broken Z_{18} symmetry shapes a hierarchical structure of the SM charged fermion mass matrices which is crucial for a natural explanation of the SM charged fermion mass and quark mixing pattern.

The fermion sector includes three SM singlets, $Z_2^{(1)}$ charged Right-Handed (RH) neutrinos N_{iR} in addition to the SM fermions. All the fermions are arranged as trivial singlets of $\Delta(27)$ with the exception of the charged leptons fields, where the $SU(2)_L$ doublets l_L transform as an anti-triplet and the l_{iR} transform as specific non-trivial singlets. The quark and lepton assignments under the $\Delta(27) \times Z_2^{(1)} \times Z_2^{(2)} \times Z_2^{(3)} \times Z_{18}$ discrete group are shown in Tables II and III, respectively.

We stress here that, thanks to the preserved $Z_2^{(1)}$ symmetry, the scalar and fermion sectors of our model contain stable DM candidates. The scalar DM candidate is the lightest among the CP-even and CP-odd neutral components of the $SU(2)$ scalar doublet h . The fermionic DM candidate corresponds to the lightest among the RH Majorana neutrinos. It is worth mentioning that in the scenario of a scalar DM candidate, it annihilates mainly into WW , ZZ , $t\bar{t}$, $b\bar{b}$ and $h_{SM}h_{SM}$ via a Higgs portal scalar interaction. These annihilation channels will contribute to the DM relic density, which can be accommodated for appropriate values of the scalar DM mass and of the coupling of the Higgs portal scalar interaction. Thus, for the DM direct detection prospects, the scalar DM candidate would scatter off a nuclear target in a detector via Higgs boson exchange in the t -channel, giving rise to a constraint on the Higgs portal scalar interaction coupling. For the fermionic DM candidate, the lightest RH neutrino, the DM relic abundance can be obtained through freeze-in, as shown in [27]. The DM constraints can therefore be fulfilled in our model for an appropriate region of parameter space, along similar lines of Refs. [27, 35–51, 66]. A detailed study of the implications of the DM candidates in our model is nevertheless beyond the scope of this work.

With the particle content previously described, the scalar potential, as well as the Yukawa terms of up quarks, down quarks, charged leptons and the neutrino terms are constrained by the symmetries, which we consider in detail in the following Sections.

III. THE LOW ENERGY SCALAR POTENTIAL

The pattern of VEVs that we consider is

$$\begin{aligned} \langle H \rangle &= v_H (0, 0, 1), & \langle \phi_1 \rangle &= v_1 (1, 0, 0), & \langle \phi_3 \rangle &= v_3 (0, 0, 1), \\ \langle \phi_{123} \rangle &= v_{123} (1, \omega, \omega^2), & \langle \phi_{23} \rangle &= v_{23} (0, 1, -1), & \langle \sigma \rangle &= v_\sigma \sim \lambda \Lambda, \end{aligned} \quad (2)$$

$$(3)$$

with $v_H = \frac{v}{\sqrt{2}}$, being $v = 246$ GeV, and $\lambda \simeq 0.225$ the Cabibbo angle. We do not consider here in detail the potential terms that give rise to the flavon VEVs. The special $\Delta(27)$ VEV directions shown above and used in our model have been obtained in the literature in the framework of Supersymmetric models with $\Delta(27)$ family symmetry through D-term alignment mechanism [2] or F-term alignment mechanism [19]. Such VEV patterns have also been derived in non-supersymmetric models and have shown to be consistent with the scalar potential minimization equations for a large region of parameter space, as discussed in detail in [23, 25, 30] (see also [67, 68]).

For the low energy scalar potential, we consider that the flavons have been integrated out, and write the scalar potential in four parts

$$V = V_H + V_h + V_{Hh} + V_{Hh}^{breaking}. \quad (4)$$

We write the $\Delta(27)$ -invariant potential for H in the notation of [67, 68]

$$\begin{aligned}
V(H) = & -\mu_H^2 \sum_{i,\alpha} H_{i\alpha} H^{*i\alpha} + s \sum_{i,\alpha,\beta} (H_{i\alpha} H^{*i\alpha})(H_{i\beta} H^{*i\beta}) \\
& + \sum_{i,j,\alpha,\beta} [r_1 (H_{i\alpha} H^{*i\alpha})(H_{j\beta} H^{*j\beta}) + r_2 (H_{i\alpha} H^{*i\beta})(H_{j\beta} H^{*j\alpha})] \\
& + \sum_{\alpha,\beta} [d (H_{1\alpha} H_{1\beta} H^{*2\alpha} H^{*3\beta} + \text{cycl.}) + \text{h.c.}] ,
\end{aligned} \tag{5}$$

where the Greek letters denote the $SU(2)_L$ indices. An equivalent way of writing $V(H)$ where the $\Delta(27)$ invariance is more transparent is shown in Appendix B.

The potential for the unbroken $Z_2^{(1)}$ -odd field h is simply

$$V_h = \mu_h^2 (hh^\dagger) + \gamma_1 (hh^\dagger)^2 , \tag{6}$$

whereas the terms mixing h and the $\Delta(27)$ triplet H are

$$V_{Hh} = \alpha_1 (HH^\dagger)_{\mathbf{10},0} (hh^\dagger) + \alpha_2 ((Hh^\dagger) (H^\dagger h))_{\mathbf{10},0} , \tag{7}$$

and expand to

$$V_{Hh} = \alpha_1 (H_1 H_1^\dagger + H_2 H_2^\dagger + H_3 H_3^\dagger) (hh^\dagger) + \alpha_2 [(H_1 h^\dagger) (H_1^\dagger h) + (H_2 h^\dagger) (H_2^\dagger h) + (H_3 h^\dagger) (H_3^\dagger h)] . \tag{8}$$

We also consider higher order terms allowed by the symmetries, even though they are suppressed. In these, we find the leading order contribution to the mass splitting between the CP-even and CP-odd neutral components of h , arises from the terms:

$$V_{Hh}^{\text{breaking}} = \kappa_1 [(H^\dagger h) (H^\dagger h)]_{\bar{\mathbf{3}}_{s_1}} \frac{\phi_{123}}{\Lambda} + \kappa_2 [(H^\dagger h) (H^\dagger h)]_{\bar{\mathbf{3}}_{s_2}} \frac{\phi_{123}}{\Lambda} + \text{h.c.} . \tag{9}$$

We present these terms as the splitting of the masses is needed in order to obtain viable neutrino masses through the radiative seesaw mechanism (see Section IV B). Another invariant term arises by replacing ϕ_{123} by ϕ_1 , but that term does not produce the effective mass term needed to yield the mass splitting between the CP-even and CP-odd neutral components of h . From the non-renormalizable scalar interactions given in Eq. (9), using the corresponding $\Delta(27)$ breaking VEV, we obtain:

$$\begin{aligned}
V_{Hh}^{\text{breaking}} = & \beta_1 [(H_1^\dagger h) (H_1^\dagger h) + \omega (H_2^\dagger h) (H_2^\dagger h) + \omega^2 (H_3^\dagger h) (H_3^\dagger h)] \\
& + \beta_2 [(H_2^\dagger h) (H_3^\dagger h) + \omega (H_1^\dagger h) (H_3^\dagger h) + \omega^2 (H_1^\dagger h) (H_2^\dagger h)] + \text{h.c.},
\end{aligned} \tag{10}$$

where $\beta_i \equiv \kappa_i v_{123}/\Lambda$.

The electroweak symmetry is spontaneously broken by the non-zero VEV of the third component of the $\Delta(27)$ scalar triplet, H_3 . After that, three electrically charged and seven neutral Higgs fields arise. The latter correspond to three CP-even (s_1^0, s_2^0, s_3^0), two CP-odd (p_1^0 and p_2^0) and two CP-mixed states (h_1^0 and h_2^0). At tree-level, the light and heavy scalars and pseudoscalars, arising from the mixing of the neutral components of H_1 and H_2 , are degenerate in mass:

$$m_{s_1^0, s_2^0}^2 = m_{p_1^0, p_2^0}^2 = v^2 \left(r_1 + r_2 - s \mp \frac{d}{2} \right) , \tag{11}$$

where the tadpole relation,

$$\frac{dV}{dH_3^0} = -\mu_H^2 v + s v^3 = 0 , \tag{12}$$

has been taken into account. As H_3 gets the non-zero VEV, it does not mix with the first and second components of H . As usual, its CP-odd and charged component are absorbed by the gauge bosons, which acquire masses, and a neutral massive scalar appears. We identify it with the SM-like Higgs boson of mass 125 GeV:

$$m_{h_{\text{SM}}}^2 \equiv m_{s_3^0}^2 = 2 s v^2 . \tag{13}$$

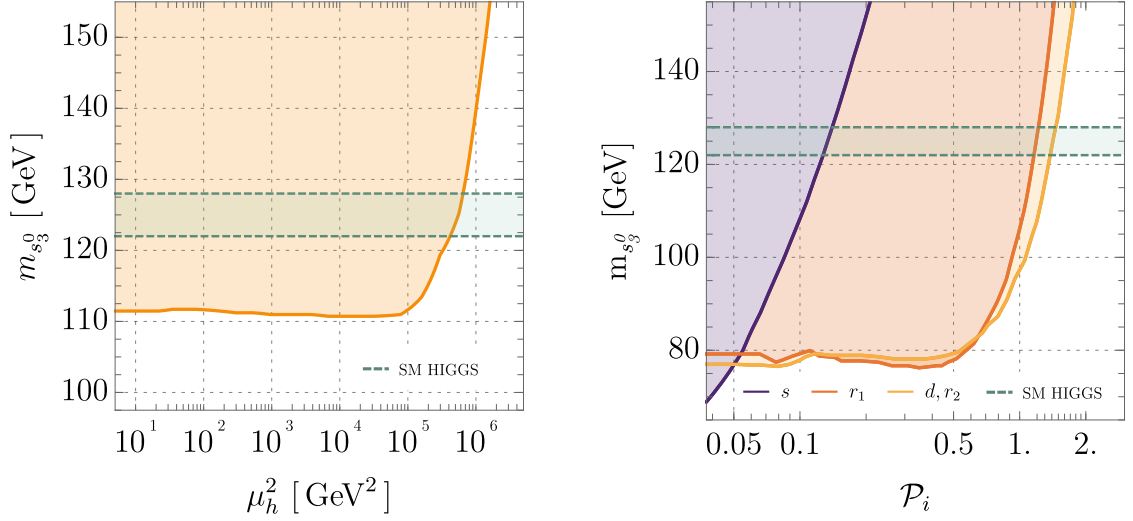


Figure 1: Loop corrected masses versus the parameters of the scalar potential in Eq (5): μ_h^2 (Left) and $\mathcal{P}_i = s, r_1, r_2, d$ (Right). The rectangular green band corresponds to the allowed values of the 125 GeV SM like Higgs boson; an uncertainty of 3 GeV is assumed in the numerical computation of the Higgs mass.

The CP-mixed neutral states are related to the $\Delta(27)$ singlet, whose squared mass matrix is:

$$\mathcal{M}_h^2 = \begin{pmatrix} \mu_h^2 + \frac{v^2}{2} (\alpha_1 + \alpha_2 - \beta_1) & \beta_1 v^2 \sin \frac{\pi}{3} \\ \beta_1 v^2 \sin \frac{\pi}{3} & \mu_h^2 + \frac{v^2}{2} (\alpha_1 + \alpha_2 + \beta_1) \end{pmatrix}. \quad (14)$$

As follows from Eq. (14), the mixing between the scalar and pseudoscalar components of h is proportional to β_1 and, therefore, negligible if $\mu_h^2 \gg \beta_1 v^2 \sin \pi/3$. At tree-level, the eigenmasses are

$$m_{h_1^0, h_2^0}^2 = \mu_h^2 + \frac{v^2}{2} (\alpha_1 + \alpha_2 \mp 2\beta_1). \quad (15)$$

The phenomenology of the model is analysed by implementing it in SARAH 4.0.4 [69–74] and generating the corresponding SPheno code [75, 76], through which the numerical simulation in Section V is performed. In particular, loop corrections are taken into account to compute the spectrum of the model. They are specially important for the SM-like Higgs, s_3^0 , whose mass is very sensitive to radiative corrections from other scalars. In Figure 1, the loop-corrected mass of this scalar is represented against the parameters of the scalar potential in Eq (5): μ_h^2, s, r_1, r_2 and d . The coloured regions correspond to the parameter space of our model. The green band reflects a theoretical uncertainty of 3 GeV that we consider in the estimation of the mass. As it can be observed, the requirement of reproducing the 125 GeV measured value sets non-trivial limits on some of the masses and quartic couplings in Eqs.(5) and (6):

$$\mu_h^2 \lesssim 6 \times 10^5 \text{ GeV}^2, \quad s \lesssim 0.14, \quad r_1 \lesssim 1.2, \quad r_2, d \lesssim 1.5. \quad (16)$$

The other parameters in Eqs.(7) and (9), which are not bounded by the mass of the SM-like Higgs, are varied in the general range $\mathcal{P}_i \in [0.05, 2.]$ during the numerical scan. Within those intervals, the masses of the resulting spectrum are:

$$m_{s_1^0, p_1^0} \lesssim 275 \text{ GeV}, \quad m_{s_2^0, p_2^0} \lesssim 350 \text{ GeV}, \quad m_{h_1^0, h_2^0} \lesssim 1 \text{ TeV}. \quad (17)$$

IV. FERMION MASSES AND MIXINGS

A. Quark masses and mixings

In the quark sector, due to the fields transforming as $\Delta(27)$ trivial singlets, there are several terms as the nine possible combinations of $\bar{q}_{iL}u_{jR}$ and the nine of $\bar{q}_{iL}d_{jR}$ are allowed by the symmetries. The quarks must necessarily couple to H because h is secluded to the neutrino sector through the unbroken $Z_2^{(1)}$. We present first the quark terms that involve H contracting with ϕ_3 , which eventually lead to the quark mass terms when the scalars acquire the respective VEVs (H acquiring a VEV in the third direction only):

$$\mathcal{L}_Y^{(Q)} = (\bar{q}_{1L} \bar{q}_{2L} \bar{q}_{3L}) \begin{pmatrix} y_{11}^{(U)} \frac{\sigma^8}{\Lambda^8} & y_{12}^{(U)} \frac{\sigma^6}{\Lambda^6} & y_{13}^{(U)} \frac{\sigma^4}{\Lambda^4} \\ y_{21}^{(U)} \frac{\sigma^6}{\Lambda^6} & y_{22}^{(U)} \frac{\sigma^4}{\Lambda^4} & y_{23}^{(U)} \frac{\sigma^2}{\Lambda^2} \\ y_{31}^{(U)} \frac{\sigma^4}{\Lambda^4} & y_{23}^{(U)} \frac{\sigma^2}{\Lambda^2} & y_{33}^{(U)} \end{pmatrix} \frac{1}{\Lambda} (\phi_3^* \tilde{H})_{\mathbf{1}_{0,0}} \begin{pmatrix} u_{1R} \\ u_{2R} \\ u_{3R} \end{pmatrix} \quad (18)$$

$$+ (\bar{q}_{1L} \bar{q}_{2L} \bar{q}_{3L}) \begin{pmatrix} y_{11}^{(D)} \frac{\sigma^7}{\Lambda^7} & y_{12}^{(D)} \frac{\sigma^6}{\Lambda^6} & y_{13}^{(D)} \frac{\sigma^6}{\Lambda^6} \\ y_{21}^{(D)} \frac{\sigma^6}{\Lambda^6} & y_{22}^{(D)} \frac{\sigma^5}{\Lambda^5} & y_{23}^{(D)} \frac{\sigma^5}{\Lambda^5} \\ y_{31}^{(D)} \frac{\sigma^4}{\Lambda^4} & y_{23}^{(D)} \frac{\sigma^3}{\Lambda^3} & y_{33}^{(D)} \frac{\sigma^3}{\Lambda^3} \end{pmatrix} \frac{1}{\Lambda} (\phi_3 H)_{\mathbf{1}_{0,0}} \begin{pmatrix} d_{1R} \\ d_{2R} \\ d_{3R} \end{pmatrix} + \text{h.c.} \quad (19)$$

The remaining quark terms have H coupling to ϕ_{123} or ϕ_1 (instead of coupling to ϕ_3):

$$\delta \mathcal{L}_Y^{(Q)} = (\bar{q}_{1L} \bar{q}_{2L} \bar{q}_{3L}) \begin{pmatrix} x_{11}^{(U)} \frac{\sigma^8}{\Lambda^8} & x_{12}^{(U)} \frac{\sigma^6}{\Lambda^6} & x_{13}^{(U)} \frac{\sigma^4}{\Lambda^4} \\ x_{21}^{(U)} \frac{\sigma^6}{\Lambda^6} & x_{22}^{(U)} \frac{\sigma^4}{\Lambda^4} & x_{23}^{(U)} \frac{\sigma^2}{\Lambda^2} \\ x_{31}^{(U)} \frac{\sigma^4}{\Lambda^4} & x_{23}^{(U)} \frac{\sigma^2}{\Lambda^2} & x_{33}^{(U)} \end{pmatrix} \sum_{r=S_1, S_2, A} \frac{c_r^{(U)}}{\Lambda^2} (\phi_{123} \tilde{H})_{\mathbf{3}_r} \phi_3 \begin{pmatrix} u_{1R} \\ u_{2R} \\ u_{3R} \end{pmatrix} \quad (20)$$

$$+ (\bar{q}_{1L} \bar{q}_{2L} \bar{q}_{3L}) \begin{pmatrix} x_{11}^{(D)} \frac{\sigma^7}{\Lambda^7} & x_{12}^{(D)} \frac{\sigma^6}{\Lambda^6} & x_{13}^{(D)} \frac{\sigma^6}{\Lambda^6} \\ x_{21}^{(D)} \frac{\sigma^6}{\Lambda^6} & x_{22}^{(D)} \frac{\sigma^5}{\Lambda^5} & x_{23}^{(D)} \frac{\sigma^5}{\Lambda^5} \\ x_{31}^{(D)} \frac{\sigma^4}{\Lambda^4} & x_{23}^{(D)} \frac{\sigma^3}{\Lambda^3} & x_{33}^{(D)} \frac{\sigma^3}{\Lambda^3} \end{pmatrix} \sum_{r=S_1, S_2, A} \frac{c_r^{(D)}}{\Lambda^2} (\phi_{123}^* H)_{\mathbf{3}_r} \phi_3^* \begin{pmatrix} d_{1R} \\ d_{2R} \\ d_{3R} \end{pmatrix} \quad (21)$$

$$+ (\phi_{123} \rightarrow \phi_1) + \text{h.c.},$$

where the r subscript denotes the possible $\Delta(27)$ representation and

$$\begin{aligned} (\phi_{123} \tilde{H})_{\mathbf{3}_{S_1}} &\supset (\tilde{H}_1, \omega \tilde{H}_2, \omega^2 \tilde{H}_3) v_{123}, & (\phi_1 \tilde{H})_{\mathbf{3}_{S_1}} &\supset (\tilde{H}_1, 0, 0) v_1, \\ (\phi_{123} \tilde{H})_{\mathbf{3}_{S_2}} &\supset (\omega \tilde{H}_3 + \omega^2 \tilde{H}_2, \omega^2 \tilde{H}_1 + \tilde{H}_3, \tilde{H}_2 + \omega \tilde{H}_1) v_{123}, & (\phi_1 \tilde{H})_{\mathbf{3}_{S_2}} &\supset (0, \tilde{H}_3, \tilde{H}_2) v_1, \\ (\phi_{123} \tilde{H})_{\mathbf{3}_A} &\supset (\omega \tilde{H}_3 - \omega^2 \tilde{H}_2, \omega^2 \tilde{H}_1 - \tilde{H}_3, \tilde{H}_2 - \omega \tilde{H}_1) v_{123}, & (\phi_1 \tilde{H})_{\mathbf{3}_A} &\supset (0, \tilde{H}_3, \tilde{H}_2) v_1. \end{aligned} \quad (22)$$

Similar products arise from $(\phi_{123}^* H)_{\mathbf{3}_r}$ with the conjugation $\omega \leftrightarrow \omega^2$.

After symmetry breaking, these terms lead to another contribution to the masses (which can be absorbed into the previous terms, as the structure is exactly the same), but also to Yukawa couplings to the other components of H . In the absence of these terms, we would have in place a Natural Flavour Conservation mechanism as only H_3 couples

to the quarks, and no FCNCs from the neutral scalars. But with these terms, we have Yukawa couplings to H_1 and H_2 . While they have the same overall texture as the mass terms, they have different coefficients, and therefore are only approximately diagonalized when going to the mass basis of the quarks. They are therefore a source of FCNCs which is controlled by the symmetries. Explicitly, the mass matrices and Yukawa couplings take the forms

$$M_U = \frac{v}{\sqrt{2}} \frac{v_3}{\Lambda} \begin{pmatrix} y_{11}^{(U)} \lambda^8 & y_{12}^{(U)} \lambda^6 & y_{13}^{(U)} \lambda^4 \\ y_{21}^{(U)} \lambda^6 & y_{22}^{(U)} \lambda^4 & y_{23}^{(U)} \lambda^2 \\ y_{31}^{(U)} \lambda^4 & y_{32}^{(U)} \lambda^2 & y_{33}^{(U)} \end{pmatrix}, \quad M_D = \frac{v}{\sqrt{2}} \frac{v_3}{\Lambda} \begin{pmatrix} y_{11}^{(D)} \lambda^7 & y_{12}^{(D)} \lambda^6 & y_{13}^{(D)} \lambda^6 \\ y_{21}^{(D)} \lambda^6 & y_{22}^{(D)} \lambda^5 & y_{23}^{(D)} \lambda^5 \\ y_{31}^{(D)} \lambda^4 & y_{32}^{(D)} \lambda^3 & y_{33}^{(D)} \lambda^3 \end{pmatrix}, \quad (23)$$

$$Y_{H_1^0}^{(U)} = \omega \lambda_{H_1^0}^{(U)} \begin{pmatrix} x_{11}^{(U)} \lambda^8 & x_{12}^{(U)} \lambda^6 & x_{13}^{(U)} \lambda^4 \\ x_{21}^{(U)} \lambda^6 & x_{22}^{(U)} \lambda^4 & x_{23}^{(U)} \lambda^2 \\ x_{31}^{(U)} \lambda^4 & x_{32}^{(U)} \lambda^2 & x_{33}^{(U)} \end{pmatrix}, \quad Y_{H_1^0}^{(D)} = \omega^2 \lambda_{H_1^0}^{(D)} \begin{pmatrix} x_{11}^{(D)} \lambda^7 & x_{12}^{(D)} \lambda^6 & x_{13}^{(D)} \lambda^6 \\ x_{21}^{(D)} \lambda^6 & x_{22}^{(D)} \lambda^5 & x_{23}^{(D)} \lambda^5 \\ x_{31}^{(D)} \lambda^4 & x_{32}^{(D)} \lambda^3 & x_{33}^{(D)} \lambda^3 \end{pmatrix}, \quad (24)$$

$$Y_{H_2^0}^{(U)} = \lambda_{H_2^0}^{(U)} \begin{pmatrix} x_{11}^{(U)} \lambda^8 & x_{12}^{(U)} \lambda^6 & x_{13}^{(U)} \lambda^4 \\ x_{21}^{(U)} \lambda^6 & x_{22}^{(U)} \lambda^4 & x_{23}^{(U)} \lambda^2 \\ x_{31}^{(U)} \lambda^4 & x_{32}^{(U)} \lambda^2 & x_{33}^{(U)} \end{pmatrix}, \quad Y_{H_2^0}^{(D)} = \lambda_{H_2^0}^{(D)} \begin{pmatrix} x_{11}^{(D)} \lambda^7 & x_{12}^{(D)} \lambda^6 & x_{13}^{(D)} \lambda^6 \\ x_{21}^{(D)} \lambda^6 & x_{22}^{(D)} \lambda^5 & x_{23}^{(D)} \lambda^5 \\ x_{31}^{(D)} \lambda^4 & x_{32}^{(D)} \lambda^3 & x_{33}^{(D)} \lambda^3 \end{pmatrix}, \quad (25)$$

$$\delta Y_{H_3^0}^{(U)} = \omega^2 \lambda_{H_3^0}^{(U)} \begin{pmatrix} x_{11}^{(U)} \lambda^8 & x_{12}^{(U)} \lambda^6 & x_{13}^{(U)} \lambda^4 \\ x_{21}^{(U)} \lambda^6 & x_{22}^{(U)} \lambda^4 & x_{23}^{(U)} \lambda^2 \\ x_{31}^{(U)} \lambda^4 & x_{32}^{(U)} \lambda^2 & x_{33}^{(U)} \end{pmatrix}, \quad \delta Y_{H_3^0}^{(D)} = \omega \lambda_{H_3^0}^{(D)} \begin{pmatrix} x_{11}^{(D)} \lambda^7 & x_{12}^{(D)} \lambda^6 & x_{13}^{(D)} \lambda^6 \\ x_{21}^{(D)} \lambda^6 & x_{22}^{(D)} \lambda^5 & x_{23}^{(D)} \lambda^5 \\ x_{31}^{(D)} \lambda^4 & x_{32}^{(D)} \lambda^3 & x_{33}^{(D)} \lambda^3 \end{pmatrix}, \quad (26)$$

where it is convenient to introduce the global effective couplings as

$$\lambda_{H_1^0}^{(U,D)} = \frac{v_3}{\sqrt{2}\Lambda^2} \left(c_{S_2}^{(U,D)} - c_A^{(U,D)} \right), \quad \lambda_{H_2^0}^{(U,D)} = \frac{v_3}{\sqrt{2}\Lambda^2} \left[\left(c_{S_2}^{(U,D)} + c_A^{(U,D)} \right) + \frac{v_1}{v_{123}} \right], \quad \lambda_{H_3^0}^{(U,D)} = \frac{v_3}{\sqrt{2}\Lambda^2} c_{S_1}^{(U,D)}. \quad (27)$$

We note again that the textures are the same for the Yukawa couplings and the mass matrices, but with different coefficients, such that the Yukawa couplings to H_1 and H_2 are not diagonalized in the quark mass basis.

The quark masses and mixings are governed by the parameters $y_{ij}^{(U,D)}$. The parameters that govern the FCNCs in the quark sector are $x_{ij}^{(U,D)}$, $c_{S_2,A}^{(U,D)}$ and they give subleading contributions to the SM quark mass matrices. Given the structure of the Yukawa couplings we do not consider our model to be predictive in the quark sector, beyond accounting for the hierarchies between the masses. The physical observables of the quark sector, i.e., the quark masses, CKM parameters and Jaroskog invariant [77, 78] can be very well reproduced in terms of natural parameters of order one. This is shown in Table IV, which for each observable, compares the model value with the respective experimental value.

The model values above are obtained from the following benchmark point:

$$M_U = \begin{pmatrix} -0.00111287 & 0.00224708 & 0.276781 \\ 0.00214193 & -0.621473 & -0.860806 \\ 0.0434745 & 0.849889 & 173.079 \end{pmatrix} \text{ GeV},$$

$$M_D = \begin{pmatrix} 0.00396153 & 0.0120505 & -0.000101736 - 0.0100846i \\ 0.00331057 & 0.0648106 & 0.0952388 \\ -0.0480789 & 0.325728 & 2.82949 \end{pmatrix} \text{ GeV}. \quad (28)$$

Observable	Model value	Experimental value
$m_u[\text{MeV}]$	1.52	1.24 ± 0.22
$m_c[\text{GeV}]$	0.63	0.63 ± 0.02
$m_t[\text{GeV}]$	172.7	172.9 ± 0.4
$m_d[\text{MeV}]$	2.88	2.69 ± 0.19
$m_s[\text{MeV}]$	55.2	53.5 ± 4.6
$m_b[\text{GeV}]$	2.86	2.86 ± 0.03
$\sin \theta_{12}^q$	0.22627	0.22650 ± 0.00048
$\sin \theta_{23}^q$	0.04077	$0.04053^{+0.00083}_{-0.00061}$
$\sin \theta_{13}^q$	0.00369	$0.00361^{+0.00009}_{-0.00011}$
J_q	3.05×10^{-5}	$(3.00^{+0.15}_{-0.09}) \times 10^{-5}$

Table IV: Model and experimental values of the quark masses and CKM parameters.

B. Lepton masses and mixings

In the lepton sector, the number of Yukawa terms is much smaller due to the assignments under $\Delta(27)$. The charged lepton and neutrino Yukawa terms invariant under the symmetries of the model are given by:

$$\mathcal{L}_Y^{(l)} = y_1^{(l)} \frac{\sigma^9}{\Lambda^9} (\bar{l}_L H)_{\mathbf{1}_{0,2}} l_{1R} + y_2^{(l)} \frac{\sigma^5}{\Lambda^5} (\bar{l}_L H)_{\mathbf{1}_{0,1}} l_{2R} + y_3^{(l)} \frac{\sigma^3}{\Lambda^3} (\bar{l}_L H)_{\mathbf{1}_{0,0}} l_{3R} + \text{h.c.} \quad , \quad (29)$$

$$\mathcal{L}_Y^{(\nu)} = y_1^{(\nu)} \frac{1}{\Lambda} (\bar{l}_L \phi_1^* \tilde{h})_{\mathbf{1}_{0,0}} N_{1R} + y_2^{(\nu)} \frac{1}{\Lambda} (\bar{l}_L \phi_{123}^* \tilde{h})_{\mathbf{1}_{0,0}} N_{2R} \quad (30)$$

$$+ y_3^{(\nu)} \frac{1}{\Lambda} (\bar{l}_L \phi_{123}^* \tilde{h})_{\mathbf{1}_{0,0}} N_{1R} + y_4^{(\nu)} \frac{1}{\Lambda} (\bar{l}_L \phi_1^* \tilde{h})_{\mathbf{1}_{0,0}} N_{2R} + y_5^{(\nu)} \frac{1}{\Lambda} (\bar{l}_L \phi_{23}^* \tilde{h})_{\mathbf{1}_{0,0}} N_{3R} \quad (31)$$

$$+ \frac{m_{N_1}}{2} \bar{N}_{1R} N_{1R}^c + \frac{m_{N_2}}{2} \bar{N}_{2R} N_{2R}^c + \frac{m_{N_3}}{2} \bar{N}_{3R} N_{3R}^c + \frac{m_{N_4}}{2} (\bar{N}_{1R} N_{2R}^c + \bar{N}_{2R} N_{1R}^c) + \text{h.c.} \quad , \quad (32)$$

where the dimensionless couplings in Eqs. (29)-(30) are $\mathcal{O}(1)$ parameters.

From the charged lepton terms and the VEV pattern we consider (see Eq. (3)), we obtain a diagonal mass matrix:

$$M_l = \begin{pmatrix} m_e & 0 & 0 \\ 0 & m_\mu & 0 \\ 0 & 0 & m_\tau \end{pmatrix}. \quad (33)$$

with the charged lepton masses given by:

$$m_e = y_1^{(l)} \frac{v v_\sigma^9}{\sqrt{2} \Lambda^9} = y_1^{(l)} \lambda^9 \frac{v}{\sqrt{2}}, \quad m_\mu = y_2^{(l)} \frac{v v_\sigma^5}{\sqrt{2} \Lambda^5} = y_2^{(l)} \lambda^5 \frac{v}{\sqrt{2}}, \quad m_\tau = y_3^{(l)} \frac{v v_\sigma^3}{\sqrt{2} \Lambda^3} = y_3^{(l)} \lambda^3 \frac{v}{\sqrt{2}}, \quad (34)$$

where in a slight abuse of notation, we have absorbed the $\mathcal{O}(1)$ parameters of the VEVs into redefinitions of $y_1^{(l)}$, $y_2^{(l)}$ and $y_3^{(l)}$ in the expressions with λ . $y_1^{(l)}$, $y_2^{(l)}$ and $y_3^{(l)}$ are assumed to be real. As in the quark sector, the Lagrangian in Eq.(29) gives rise to FCNCs through additional Yukawa couplings that arise with the other components of H , namely H_1 and H_2 . The entries are of the same size of those in $Y_{H_3}^{(l)}$ but in different positions, thus

$$Y_{H_1}^{(l)} = \frac{\sqrt{2}}{v} \begin{pmatrix} 0 & 0 & m_\tau \\ m_e & 0 & 0 \\ 0 & m_\mu & 0 \end{pmatrix}, \quad Y_{H_2}^{(l)} = \frac{\sqrt{2}}{v} \begin{pmatrix} 0 & m_\mu & 0 \\ 0 & 0 & m_\tau \\ m_e & 0 & 0 \end{pmatrix}. \quad (35)$$

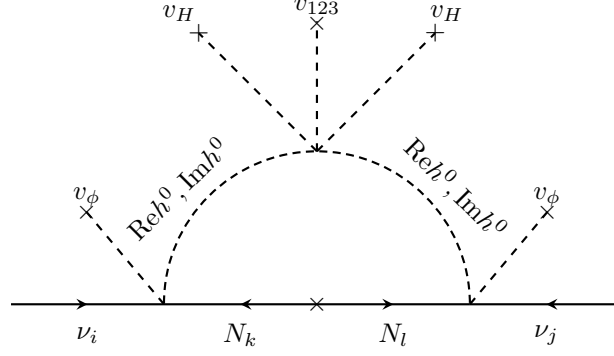


Figure 2: One-loop Feynman diagram contributing to the light active neutrino mass matrix. Here $i, j, k, l = 1, 2, 3$ and v_ϕ stands for either v_1 , v_{23} or v_{123} .

In the neutrino sector, sorting out the products in Eq. (30-32), the Yukawa and Majorana mass matrices display the following structures:

$$Y_\nu = \frac{1}{\sqrt{2}\Lambda} \begin{pmatrix} y_3^{(\nu)} v_{123} + y_1^{(\nu)} v_1 & y_2^{(\nu)} v_{123} + y_4^{(\nu)} v_1 & 0 \\ \omega^2 y_3^{(\nu)} v_{123} & \omega^2 y_2^{(\nu)} v_{123} & y_5^{(\nu)} v_{23} \\ \omega y_3^{(\nu)} v_{123} & \omega y_2^{(\nu)} v_{123} & -y_5^{(\nu)} v_{23} \end{pmatrix}, \quad M_N = \begin{pmatrix} m_{N_1} & m_{N_4} & 0 \\ m_{N_4} & m_{N_2} & 0 \\ 0 & 0 & m_{N_3} \end{pmatrix}. \quad (36)$$

After the spontaneous breaking of the discrete symmetries and of the electroweak symmetry, the following neutrino Yukawa interactions arise:

$$\begin{aligned} \mathcal{L}_Y^{(\nu)} &= z_1^{(\nu)} \bar{\nu}_{1L} (h_R^0 - i h_I^0) \tilde{N}_{1R} + z_2^{(\nu)} (\omega^2 \bar{\nu}_{2L} + \omega \bar{\nu}_{3L}) (h_R^0 - i h_I^0) \tilde{N}_{1R} \\ &+ z_3^{(\nu)} \bar{\nu}_{1L} (h_R^0 - i h_I^0) \tilde{N}_{2R} + z_4^{(\nu)} (\omega^2 \bar{\nu}_{2L} + \omega \bar{\nu}_{3L}) (h_R^0 - i h_I^0) \tilde{N}_{2R} + z_5^{(\nu)} (\bar{\nu}_{2L} - \bar{\nu}_{3L}) (h_R^0 - i h_I^0) N_{3R} \\ &+ \frac{m_{\tilde{N}_1}}{2} \tilde{N}_{1R} \tilde{N}_{1R}^c + \frac{m_{\tilde{N}_2}}{2} \tilde{N}_{2R} \tilde{N}_{2R}^c + \frac{m_{N_3}}{2} \bar{N}_{3R} N_{3R}^c + \text{h.c.}, \end{aligned} \quad (37)$$

with $m_{h_R^0} = m_{\text{Re}[h^0]}$ and $m_{h_I^0} = m_{\text{Im}[h^0]}$, while \tilde{N}_{1R} , \tilde{N}_{2R} are the physical Majorana neutrino fields arising from the combinations of N_{1R} and N_{2R} . They are given by:

$$\begin{pmatrix} \tilde{N}_{1R} \\ \tilde{N}_{2R} \end{pmatrix} = \begin{pmatrix} \cos \beta & -\sin \beta \\ \sin \beta & \cos \beta \end{pmatrix} \begin{pmatrix} N_{1R} \\ N_{2R} \end{pmatrix} \quad (38)$$

where the mixing angle β takes the form $\tan 2\beta = -2m_{N_4}/(m_{N_1} - m_{N_2})$. The $z_i^{(\nu)}$ are the Yukawa parameters in the basis of diagonal M_N obtained by performing the rotation in Eq.(38). In that basis, the neutrino Yukawa matrix ($Y_\nu \rightarrow \tilde{Y}_\nu$) maintains the structure of Eq.(36) but with new entries determined by $z_i^{(\nu)}$. The explicit expression for \tilde{Y}_ν and the relation between the $y_i^{(\nu)}$ and $z_i^{(\nu)}$ parameters is given in Appendix C. Therefore, in the basis where the RH neutrinos are diagonal, the light active neutrino mass matrix is obtained from the radiative seesaw mechanism as shown in the Feynman diagram of Figure 2 and it is given by:

$$M_\nu \equiv \frac{1}{2(4\pi)^2} \tilde{Y}_\nu \begin{pmatrix} m_{\tilde{N}_1} f_1 & 0 & 0 \\ 0 & m_{\tilde{N}_2} f_2 & 0 \\ 0 & 0 & m_{N_3} f_3 \end{pmatrix} \tilde{Y}_\nu^T, \quad (39)$$

with

$$f_k = f(m_{h_R^0}, m_{h_I^0}, m_{\tilde{N}_k}), \quad f_3 = f(m_{h_R^0}, m_{h_I^0}, m_{N_3}), \quad k = 1, 2. \quad (40)$$

The loop function f takes the form:

$$f(m_{h_R^0}, m_{h_I^0}, m_{N_R}) = \frac{m_{h_R^0}^2}{m_{h_R^0}^2 - m_{N_R}^2} \ln \left(\frac{m_{h_R^0}^2}{m_{N_R}^2} \right) - \frac{m_{h_I^0}^2}{m_{h_I^0}^2 - m_{N_R}^2} \ln \left(\frac{m_{h_I^0}^2}{m_{N_R}^2} \right), \quad (41)$$

Observable	Model value	Neutrino oscillation global fit values (NH)			
		Best fit $\pm 1\sigma$ [79]	Best fit $\pm 1\sigma$ [80]	3σ range [79]	3σ range [80]
$\Delta m_{21}^2 [10^{-5} \text{eV}^2]$	7.51	$7.50^{+0.22}_{-0.20}$	$7.42^{+0.21}_{-0.20}$	6.94 – 8.14	6.82 – 8.04
$\Delta m_{31}^2 [10^{-3} \text{eV}^2]$	2.56	$2.56^{+0.03}_{-0.04}$	$2.517^{+0.026}_{-0.028}$	2.46 – 2.65	2.435 – 2.598
$\theta_{12}^l [^\circ]$	34.45	34.3 ± 1.0	$33.44^{+0.77}_{-0.74}$	31.4 – 37.4	31.27 – 35.86
$\theta_{13}^l [^\circ]$	8.59	$8.58^{+0.11}_{-0.15}$	8.57 ± 0.12	8.16 – 8.94	8.20 – 8.93
$\theta_{23}^l [^\circ]$	44.89	$48.79^{+0.93}_{-1.25}$	$49.2^{+0.9}_{-1.2}$	41.63 – 51.32	40.1 – 51.7
$\delta_{\text{CP}} [^\circ]$	203.15	216^{+41}_{-25}	197^{+27}_{-24}	144 – 360	120 – 369

Table V: Model and experimental values of the neutrino mass squared splittings, leptonic mixing angles, and CP-violating phase. The experimental values are taken from Refs. [79, 80].

where $m_{h_R}^2, m_{h_I}^2$ are given in terms of the parameters of the scalar potential in the entries (1,1) and (2,2) of Eq. (15). One can show that the resulting light active neutrino mass matrix in Eq. (39) can be parametrized as:

$$M_\nu = \begin{pmatrix} a & d\omega^2 & d\omega \\ d\omega^2 & be^{i\theta} & c \\ d\omega & c & be^{-i\theta} \end{pmatrix}, \quad (42)$$

where the exact relations between the effective parameters a, b, c, d, θ and the lagrangian parameters $z_i^{(\nu)}$ are given in Appendix C. Here, we stress that c can be expressed in terms of b and θ , and that all the effective parameters depend on the flavon VEVs.

The masses of the charged leptons are set to the observed values, and the remaining parameters that govern the neutrino sector are $y_{1,2,3,4,5}^{(\nu)}, m_{N_{1,2,3,4}}$. The model is predictive as only the combinations a, b, c, d, θ of these parameters affect the physical observables of the neutrino sector, i.e., the three leptonic mixing angles, the CP phase and the neutrino mass squared splittings for the normal mass hierarchy (NH). These observables can be very well reproduced, as shown in Table V, starting from the following benchmark point:

$$a \simeq 10.64 \text{ meV}, \quad b \simeq 30.89 \text{ meV}, \quad c \simeq -19.79 \text{ meV}, \quad d \simeq (1.59 + i 5.83) \text{ meV}, \quad \theta \simeq 26.29^\circ. \quad (43)$$

This shows that our predictive model successfully describes the current neutrino oscillation experimental data. As c depends on b and θ , we conclude that with only four effective parameters, i.e., a, b, d and θ , we can successfully reproduce the experimental values of the six physical observables of the neutrino sector: the neutrino mass squared differences, the leptonic mixing angles and the leptonic CP phase. The correlations between neutrino observables are depicted in Figure 3, while the value of θ_{23} is almost constant. To obtain this Figure, the lepton sector parameters were randomly generated in a range of values where the neutrino mass squared splittings, leptonic mixing parameters and leptonic CP violating phase are inside the 3σ experimentally allowed range. We note also that obtaining the correct scale for the light neutrino masses (and therefore, for the effective parameters) is implicitly setting a magnitude for $v_{123,1}/\Lambda \lesssim 10^{-2}$.

Another important lepton sector observable is the effective Majorana neutrino mass parameter of the neutrinoless double beta decay, which gives us information on the Majorana nature of neutrinos. The amplitude for this process is directly proportional to the effective Majorana mass parameter, which is defined as follows:

$$m_{\beta\beta} = \left| \sum_j U_{ej}^2 m_{\nu_k} \right|, \quad (44)$$

where U_{ej} and m_{ν_k} are the PMNS leptonic mixing matrix elements and the neutrino Majorana masses, respectively. Figure 3 displays $m_{\beta\beta}$ as function of the smallest of the light active neutrino masses m_{\min} , which for the normal mass hierarchy scenario corresponds to $m_{\min} = m_{\nu 1}$. The points displayed are all consistent with the experimental

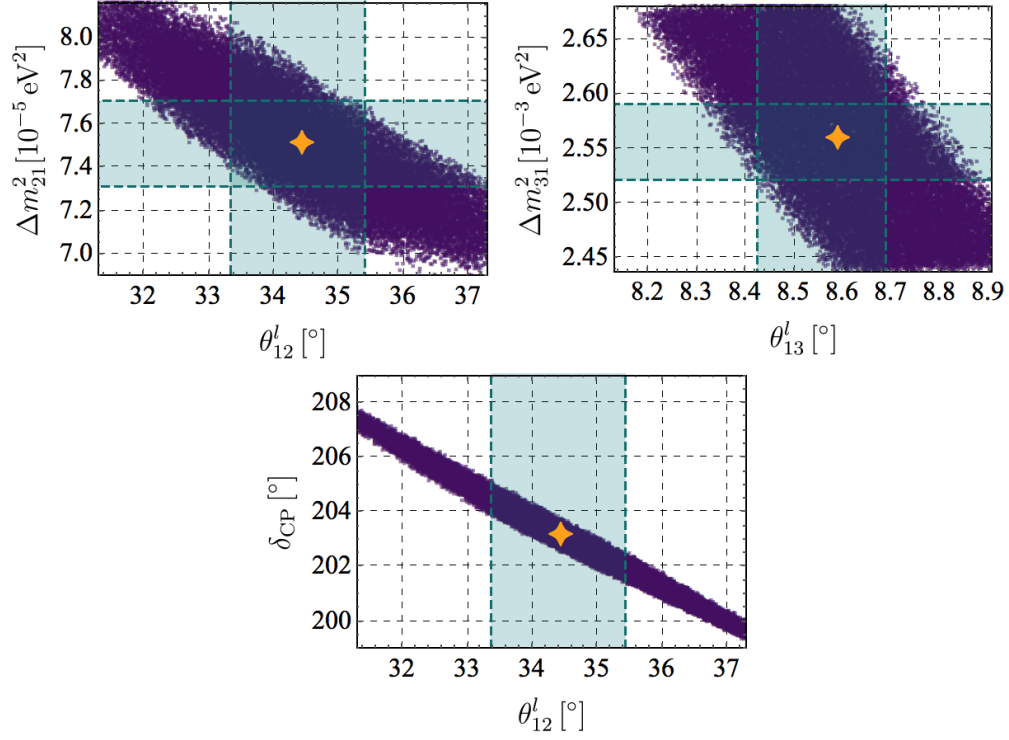


Figure 3: Correlation between neutrino observables around the benchmark point. The star corresponds to the benchmark point considered in the text, whereas the dashed lines correspond to the experimental 1σ ranges of [79].

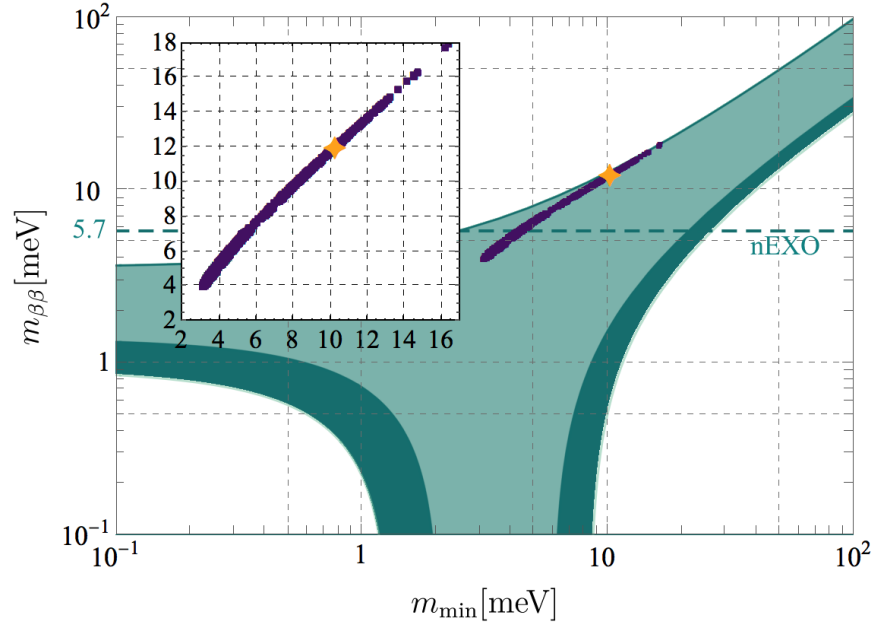


Figure 4: The effective Majorana neutrino mass parameter $m_{\beta\beta}$ against $m_{\min} = m_{\nu 1}$. The green shadow is the allowed for NO scenarios. The dashed line corresponds to the future sensitivity expected from the nEXO experiment. The inner plot zooms in the correlation between $m_{\beta\beta}$ and m_{\min} .

data with a $\chi^2 < 1.5$. We find that our model predicts the effective Majorana neutrino mass parameter in the range $m_{\beta\beta} \lesssim (3 - 18)$ meV for the case of normal hierarchy. The new limit $T_{1/2}^{0\nu\beta\beta}(^{100}\text{Mo}) \geq 1.5 \times 10^{24}$ yr on the half-life of $0\nu\beta\beta$ decay in ^{100}Mo has been recently obtained [81]. This new limit translates into a corresponding upper bound on $m_{\beta\beta} \leq (300 - 500)$ meV at 90% CL. However, it is worth mentioning that the proposed nEXO experiment [82, 83] will reach a sensitivity for the ^{136}Xe $0\nu\beta\beta$ half-life of $T_{1/2}^{0\nu\beta\beta}(^{136}\text{Xe}) \geq 9.2 \times 10^{27}$ yr at 90% CL. This can be converted into an exclusion limit on the effective Majorana neutrino mass between 5.7 meV and 17.7 meV. In the most optimistic scenario this will exclude most of the predicted region of values of our model.

V. CONSTRAINTS FROM FCNCs

Given the Yukawa couplings discussed in the previous Section for quarks and leptons, we have generically concluded that FCNCs will be present in both sectors, mediated by physical neutral Higgs fields. In this Section, we discuss in more detail how specific processes already act to constrain the parameter space of the model and highlight the near-future experiments that will further act to probe the model. To this aim, we performed a numerical simulation in SPheno considering the free input parameters of our model in the following intervals

$$\text{effective parameters : } \quad \frac{v_3}{\Lambda} \in [0.2, 0.5] \quad , \quad \frac{v_{i \neq 3}}{\Lambda} \in [10^{-3}, 0.5], \quad (45)$$

$$\text{scalar potential : } \quad \mu_h^2 \in [0, 10^6] \text{ GeV}^2 \quad , \quad r_{1,2}, d, s, \alpha_{1,2} \in [0.05, 2] \quad , \quad \beta_{1,2} \in [0.05, 2] \frac{v_{123}}{\Lambda}, \quad (46)$$

$$\text{quark sector : } \quad x_{ij}^{(U,D)}, c_{S_{2,A}}^{(U,D)} \in \pm [0.5, 1.5], \quad (47)$$

$$\text{neutrino sector : } \quad y_{1,2,3,4,5}^{(\nu)} \in [0.5, 1.5] \quad , \quad m_{N_{1,2,3,4}} \in [10^{-1}, 10^6] \text{ GeV} \quad \text{with} \quad m_{N_1} < m_{N_4} < m_{N_2} < m_{N_3}. \quad (48)$$

Despite the large number of model parameters, we recall that the neutrino sector of the model is predictive, as it depends only on 4 independent effective parameters (a, b, d, θ) . Furthermore, the effective parameters $x_{ij}^{(U,D)}$ and $c_{S_{2,A}}^{(U,D)}$ give subleading contributions to the SM quark mass matrices and thus to the quark sector observables. Those parameters are however important as they govern the FCNCs in the quark sector. The most relevant Yukawa couplings are $Y_{H_{1,2}^0}^{(U,D)}$, which we analyse through the effective coupling $\lambda_{H_{1,2}^0}^{(U,D)}$ of Eq. (27). Considering Eq. (27), upper bounds on this quantity reflect on the ratio of the flavon VEVs and the scale Λ . Due to the top quark Yukawa coupling, coming from Eq. (23), we expect $v_3/\Lambda \in [0.2, 0.5]$, therefore we interpret the upper bounds on $\lambda_{H_{1,2}^0}^{(U,D)}$ to imply a hierarchy between v_3 (larger) and v_{123}, v_1 (smaller). This hierarchy suppresses the effective couplings of Eq. (27). Notice that the value of these couplings is not constrained by the model itself, although there is a dependence of $v_{123,1}/\Lambda$ on the scale of light neutrino masses which suggests $\lambda_{H_{1,2}^0}^{(U,D)} \lesssim 5 \times 10^{-3}$.

In Figure 5 we show the dependence of the quark flavor violating observables $b \rightarrow s\gamma$ and ε_K on $\lambda_{H_{1,2}^0}^{(U,D)}$. The model prediction for these observables is displayed through ratios to their respective SM values. The narrow horizontal band indicates the limit where the experimentally allowed SM-like values are safely recovered. Figure 5 shows that $b \rightarrow s\gamma$ would constrain the value of the couplings to be below $\lambda_{H_{1,2}^0}^{(U,D)} \lesssim 0.5$ (orange points). Very similar bounds, for simplicity not displayed in the figure, come from $B_{d(s)} \rightarrow \mu^+\mu^-$ and $B_d \rightarrow \tau^+\tau^-$. Figure 5 also shows that a more constraining limit comes from the CP violating observable ε_K . We see that this observable would effectively restrict the couplings to $\lambda_{H_{1,2}^0}^{(U,D)} \lesssim 0.1$, although most of the points concentrate at $\lambda_{H_{1,2}^0}^{(U,D)} \lesssim 10^{-2}$ (orange points). In these plots, the orange and yellow points are excluded by this and other constraints, mostly the requirement to obtain the light neutrino masses. In these plots, the requirement to obtain the light neutrino masses is very restrictive and only dark purple points satisfy all the constraints.

In the leptonic sector, among the Lepton Flavour Violating (LFV) processes, the muon to electron flavour violating nuclear conversion

$$\mu^- + N(A, Z) \rightarrow e^- + N(A, Z) \quad (49)$$

is known to provide a very sensitive probe of lepton flavour violation. Currently the best upper bound on the $\mu \rightarrow e$ nuclear conversion comes from the SINDRUM II experiment [84] at PSI, using a Gold stopping target. This gives a current limit on the conversion rate of $\text{CR}(\mu^- \text{Au} \rightarrow e^- \text{Au}) < 7 \times 10^{-13}$.

Searches for $\mu \rightarrow e$ conversion at the Mu2e experiment [85] in FNAL and the proposed upgrade to COMET (Phase-II) experiment [86] in J-PARC would achieve a similar sensitivity and an upper limit of $\text{CR}(\mu^- \text{Al} \rightarrow e^- \text{Al}) < 6 \times 10^{-17}$, that is four orders of magnitude below the present bound. In the long run, the PRISM/PRIME [87] is being designed to probe values of the $\mu \rightarrow e$ conversion rate on Titanium, which is smaller by 2 orders of magnitude: $\text{CR}(\mu^- \text{Ti} \rightarrow e^- \text{Ti}) < 10^{-18}$.

We focus here on the $\mu \rightarrow e$ conversion because, contrary to the naive expectation of $\mu \rightarrow e$ nuclear conversion being proportional to $\mu \rightarrow e\gamma$, in our model we observe an interesting enhancement of the $\mu \rightarrow e$ nuclear conversion detached from other LFV processes like $\mu \rightarrow e\gamma$, $\tau \rightarrow (e, \mu)\gamma$, $\mu \rightarrow 3e$ and $\tau \rightarrow 3(e, \mu)$, which remain suppressed. In fact, from the couplings in Eqs. (29), $\mu \rightarrow e$ can be generated already at tree-level through the exchange of a neutral scalar.

Because of this, the impressive future sensitivity in this process will place significant constraints on the proposed model.

As the process also involves quarks (inside the nuclei), we find it convenient to show the observable in terms of the effective parameters $\lambda_{H_{1,2}}^{(U,D)}$ (already used in the previous Figures) in Figure 6. The orange (grey and lightest grey) points regions are already excluded by light neutrino masses, the observed value of $b \rightarrow s\gamma$ or ε_K . The dashed horizontal lines show the future limits (as discussed above). Particularly from Figure 6, We observe that a large percentage of the predicted points of the model reside in a window accessible to future experiments.

Figure 7 on the other hand shows that, while it is in theory possible to constrain the values of the RH neutrino masses through $\mu \rightarrow e\gamma$ such that it would eventually lead to lower bounds on M_2 and M_3 , in practice the values expected in our model are too small to allow this process to effectively probe the parameter space.

VI. CONCLUSIONS

In this work we presented a model based on the $\Delta(27)$ family symmetry, featuring a low energy scalar potential with 3+1 $SU(2)$ doublet scalars arranged as an anti-triplet (H) and trivial singlet (h) of the family symmetry. The latter does not acquire a Vacuum Expectation Value since it is charged under a preserved $Z_2^{(1)}$ symmetry, and is secluded in the neutrino sector, where it leads to a radiative seesaw mechanism that produces the tiny masses of the light active neutrinos.

The quarks, being singlets of $\Delta(27)$, couple to H through $\Delta(27)$ invariant combinations of H and at least one of the $\Delta(27)$ triplet flavons - one such combination giving rise to their masses and mixing through the third component H_3 (identified with the Standard Model-like Higgs), and other combinations giving rise to Yukawa couplings to $H_{1,2}$. The extra physical scalars are mixtures of $H_{1,2}$ and have off-diagonal couplings to the quarks that are controlled by the symmetries.

The $SU(2)$ doublet leptons are arranged like H as anti-triplets of $\Delta(27)$. The respective invariant combinations don't involve the triplet flavons, and include couplings to H_3 leading to the charged lepton masses and to $H_{1,2}$ yielding Flavour Changing Neutral Currents, which are nevertheless controlled by the symmetries. The specific combination of neutrino masses that originate from radiative seesaw and through invariants featuring $\Delta(27)$ triplet flavons produces the cobimaximal mixing pattern.

Our model successfully accommodates the experimental values of the quark and lepton (including neutrino) masses, mixing angles, and CP phases. Furthermore, the effective Majorana neutrino mass parameter is predicted to be in the range $3 \text{ meV} \lesssim m_{\beta\beta} \lesssim 18 \text{ meV}$ for the case of normal hierarchy. Most of the predicted range of values for the effective Majorana neutrino mass parameter is within the declared range $5.7 - 17.7 \text{ meV}$ of sensitivity of modern experiments [83].

The detailed analysis of the Flavour Changing Neutral Currents lead to strong constraints on the model parameter

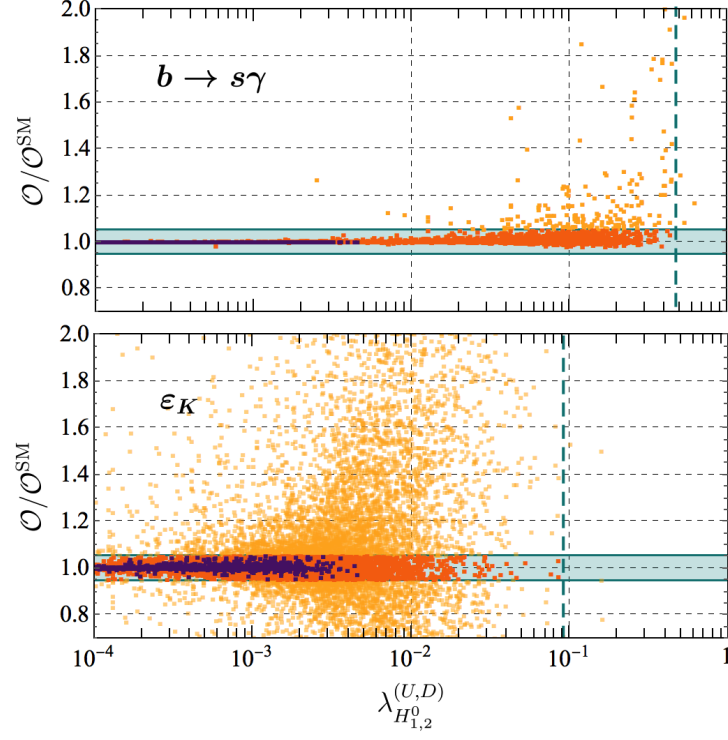


Figure 5: Limits on the effective coupling $\lambda_{H_{1,2}^0}^{(U,D)}$ (vertical dashed lines) coming from the observable $b \rightarrow s\gamma$ (top plot) and the CP observable ε_K (bottom plot) respectively. The horizontal band indicates the allowed range. Light yellow points show the full scanned region. Points that satisfy the quark observable are in orange, only dark purple points are compatible with the neutrino observables.

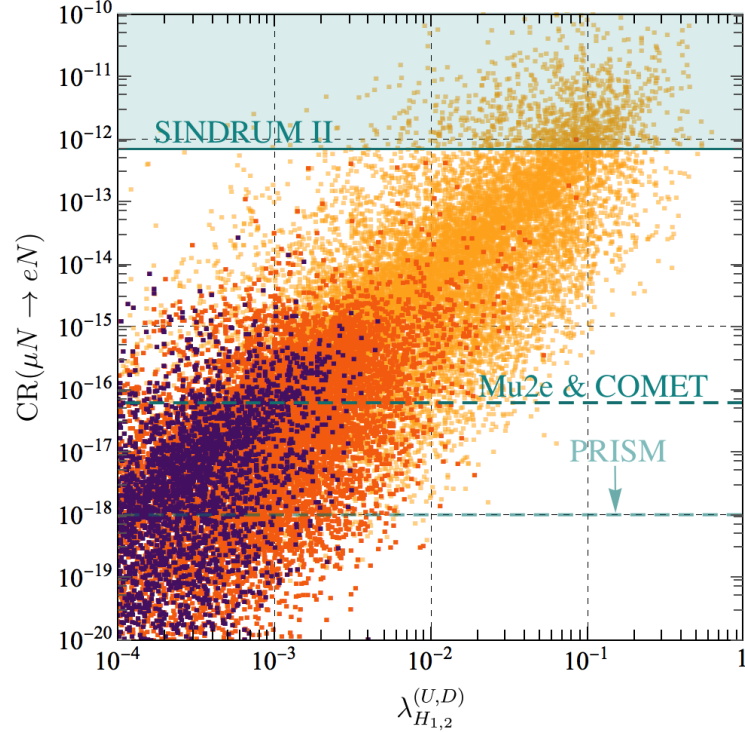


Figure 6: The LFV observable $\mu \rightarrow e$ nuclear conversion versus the effective coupling $\lambda_{H_{1,2}^0}^{(U,D)}$. The colours correspond to those of the most restrictive case of Figure 5 (bottom panel).

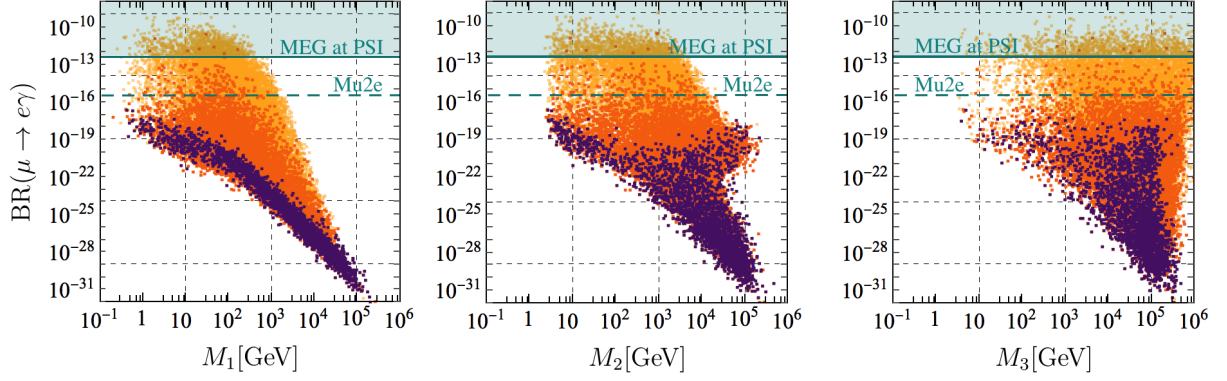


Figure 7: The LFV observable $\text{BR}(\mu \rightarrow e\gamma)$ versus the RH-neutrino masses. Here we have taken into account the lower bound of $[0.1 - 1]$ GeV on the right handed Majorana neutrino masses arising from Big Bang Nucleosynthesis (BBN) [88]. The colours correspond to those of the most restrictive case of Figure 5 (bottom panel).

space. Of particular note are $\mu \rightarrow e$ nuclear conversion processes and Kaon mixing, which already restrict the model parameter space, and that are generally predicted by the model to be in a range within the reach of future experiments.

Acknowledgments

The authors thank Avelino Vicente for very useful discussions. A.E.C.H is supported by ANID-Chile FONDECYT 1210378. IdMV acknowledges funding from Fundação para a Ciência e a Tecnologia (FCT) through the contract IF/00816/2015 and was supported in part by the National Science Center, Poland, through the HARMONIA project under contract UMO-2015/18/M/ST2/00518, and by FCT through projects CFTP-FCT Unit 777 (UID/FIS/00777/2019), PTDC/FIS-PAR/29436/2017, CERN/FIS-PAR/0004/2019 and CERN/FIS-PAR/0008/2019 which are partially funded through POCTI (FEDER), COMPETE, QREN and EU. MLLI acknowledges support from the China Postdoctoral Science Foundation No.2020M670475. AM acknowledges support by the Estonian Research Council grants PRG803 and MOBTT86, and by the EU through the European Regional Development Fund CoE program TK133 “The Dark Side of the Universe.”

Appendix A: The $\Delta(27)$ discrete group

The $\Delta(27)$ discrete group has the following 11 irreducible representations: one triplet $\mathbf{3}$, one anti-triplet $\bar{\mathbf{3}}$ and nine singlets $\mathbf{1}_{k,l}$ ($k, l = 0, 1$), where k and l correspond to the charges of two Z_3 and Z'_3 generators of this group, respectively [89]. The $\Delta(27)$ irreducible representations fulfill the following tensor product rules [89]:

$$\begin{aligned}
 \mathbf{3} \otimes \mathbf{3} &= \bar{\mathbf{3}}_{S_1} \oplus \bar{\mathbf{3}}_{S_2} \oplus \bar{\mathbf{3}}_A \\
 \bar{\mathbf{3}} \otimes \bar{\mathbf{3}} &= \mathbf{3}_{S_1} \oplus \mathbf{3}_{S_2} \oplus \mathbf{3}_A \\
 \mathbf{3} \otimes \bar{\mathbf{3}} &= \sum_{r=0}^2 \mathbf{1}_{r,0} \oplus \sum_{r=0}^2 \mathbf{1}_{r,1} \oplus \sum_{r=0}^2 \mathbf{1}_{r,2} \\
 \mathbf{1}_{k,\ell} \otimes \mathbf{1}_{k',\ell'} &= \mathbf{1}_{k+k' \bmod 3, \ell+\ell' \bmod 3}
 \end{aligned} \tag{A1}$$

Denoting (x_1, y_1, z_1) and (x_2, y_2, z_2) as the basis vectors for two $\Delta(27)$ triplets $\mathbf{3}$ (or $\bar{\mathbf{3}}$), one finds:

$$\begin{aligned}
(\mathbf{3} \otimes \mathbf{3})_{\bar{\mathbf{3}}_{S_1}} &= (x_1 y_1, x_2 y_2, x_3 y_3), \\
(\mathbf{3} \otimes \mathbf{3})_{\bar{\mathbf{3}}_{S_2}} &= \frac{1}{2} (x_2 y_3 + x_3 y_2, x_3 y_1 + x_1 y_3, x_1 y_2 + x_2 y_1), \\
(\mathbf{3} \otimes \mathbf{3})_{\bar{\mathbf{3}}_A} &= \frac{1}{2} (x_2 y_3 - x_3 y_2, x_3 y_1 - x_1 y_3, x_1 y_2 - x_2 y_1), \\
(\mathbf{3} \otimes \bar{\mathbf{3}})_{\mathbf{1}_{r,0}} &= x_1 y_1 + \omega^{2r} x_2 y_2 + \omega^r x_3 y_3, \\
(\mathbf{3} \otimes \bar{\mathbf{3}})_{\mathbf{1}_{r,1}} &= x_1 y_2 + \omega^{2r} x_2 y_3 + \omega^r x_3 y_1, \\
(\mathbf{3} \otimes \bar{\mathbf{3}})_{\mathbf{1}_{r,2}} &= x_1 y_3 + \omega^{2r} x_2 y_1 + \omega^r x_3 y_2,
\end{aligned} \tag{A2}$$

where $r = 0, 1, 2$ and $\omega = e^{i\frac{2\pi}{3}}$.

Appendix B: Scalar potential

The scalar potential for the $\Delta(27)$ triplet H can be written in the form:

$$\begin{aligned}
V_H &= -\mu_H^2 (HH^\dagger)_{\mathbf{1}_{0,0}} + \rho_1 (HH^\dagger)_{\mathbf{1}_{0,0}} (HH^\dagger)_{\mathbf{1}_{0,0}} + \rho_2 (HH^\dagger)_{\mathbf{1}_{1,0}} (HH^\dagger)_{\mathbf{1}_{2,0}} + \rho_3 (HH^\dagger)_{\mathbf{1}_{0,1}} (HH^\dagger)_{\mathbf{1}_{0,2}} \\
&\quad + \rho_4 \left[(HH^\dagger)_{\mathbf{1}_{1,1}} (HH^\dagger)_{\mathbf{1}_{2,2}} + \text{h.c.} \right].
\end{aligned} \tag{B1}$$

The following relations hold between the parameters in Eq. (5) and those in Eq. (B1):

$$s \equiv \rho_1 + \rho_2 \quad , \quad r_1 \equiv 2\rho_1 - \rho_2 \quad , \quad r_2 \equiv \rho_3 - \rho_4 \quad , \quad d \equiv \rho_3 - \omega^2 \rho_4. \tag{B2}$$

Appendix C: Neutrino mass parameters

The neutrino Yukawa matrix, in the basis of diagonal RH-neutrinos, is given by

$$\tilde{Y}_\nu = Y_\nu R_\beta^T = \frac{1}{\sqrt{2}\Lambda} \begin{pmatrix} z_1^{(\nu)} & z_3^{(\nu)} & 0 \\ z_2^{(\nu)} \omega^2 & z_4^{(\nu)} \omega^2 & z_5^{(\nu)} \\ z_2^{(\nu)} \omega & z_4^{(\nu)} \omega & -z_5^{(\nu)} \end{pmatrix}, \tag{C1}$$

where R_β refers to the rotation in Eq.(38) and the Yukawa parameters are:

$$\begin{aligned}
z_1^{(\nu)} &= \frac{1}{\sqrt{2}} \left[\left(y_3^{(\nu)} \frac{v_{123}}{\Lambda} + y_1^{(\nu)} \frac{v_1}{\Lambda} \right) \cos \beta - \left(y_2^{(\nu)} \frac{v_{123}}{\Lambda} + y_4^{(\nu)} \frac{v_1}{\Lambda} \right) \sin \beta \right], \\
z_2^{(\nu)} &= \frac{v_{123}}{\sqrt{2}\Lambda} \left(y_3^{(\nu)} \cos \beta - y_2^{(\nu)} \sin \beta \right), \\
z_3^{(\nu)} &= \frac{1}{\sqrt{2}} \left[\left(y_3^{(\nu)} \frac{v_{123}}{\Lambda} + y_1^{(\nu)} \frac{v_1}{\Lambda} \right) \sin \beta + \left(y_2^{(\nu)} \frac{v_{123}}{\Lambda} + y_4^{(\nu)} \frac{v_1}{\Lambda} \right) \cos \beta \right], \\
z_4^{(\nu)} &= \frac{v_{123}}{\sqrt{2}\Lambda} \left(y_3^{(\nu)} \sin \beta + y_2^{(\nu)} \cos \beta \right), \\
z_5^{(\nu)} &= \frac{y_5^{(\nu)} v_{23}}{\sqrt{2}\Lambda}.
\end{aligned} \tag{C2}$$

The relation between the light effective neutrino mass parameters in Eq. (42) and the lagrangian parameters z_i'' reads as

$$\begin{aligned}
a &= \frac{\left(z_1^{(\nu)}\right)^2 m_{\tilde{N}_1}}{16\pi^2} f_1 + \frac{\left(z_3^{(\nu)}\right)^2 m_{\tilde{N}_2}}{16\pi^2} f_2, \\
b &= \left| \frac{\omega \left(z_2^{(\nu)}\right)^2 m_{\tilde{N}_1}}{16\pi^2} f_1 + \frac{\omega \left(z_4^{(\nu)}\right)^2 m_{\tilde{N}_2}}{16\pi^2} f_2 + \frac{\left(z_5^{(\nu)}\right)^2 m_{N_3}}{16\pi^2} f_3 \right|, \\
c &= \frac{\left(z_2^{(\nu)}\right)^2 m_{\tilde{N}_1}}{16\pi^2} f_1 + \frac{\left(z_4^{(\nu)}\right)^2 m_{\tilde{N}_2}}{16\pi^2} f_2 - \frac{\left(z_5^{(\nu)}\right)^2 m_{N_3}}{16\pi^2} f_3, \\
d &= \frac{z_1^{(\nu)} z_2^{(\nu)} m_{\tilde{N}_1}}{16\pi^2} f_1 + \frac{z_3^{(\nu)} z_4^{(\nu)} m_{\tilde{N}_2}}{16\pi^2} f_2, \\
\theta &= \arg \left(\frac{\omega \left(z_2^{(\nu)}\right)^2 m_{\tilde{N}_1}}{16\pi^2} f_1 + \frac{\omega \left(z_4^{(\nu)}\right)^2 m_{\tilde{N}_2}}{16\pi^2} f_2 + \frac{\left(z_5^{(\nu)}\right)^2 m_{N_3}}{16\pi^2} f_3 \right),
\end{aligned} \tag{C3}$$

with f_k as defined in Eq. (40). The system admits a solution as long as $c = b(\sin \theta - \sqrt{3} \cos \theta)/\sqrt{3}$.

-
- [1] G. C. Branco, J. M. Gerard, and W. Grimus, “GEOMETRICAL T VIOLATION,” *Phys. Lett.* **136B** (1984) 383–386.
 - [2] I. de Medeiros Varzielas, S. F. King, and G. G. Ross, “Neutrino tri-bi-maximal mixing from a non-Abelian discrete family symmetry,” *Phys. Lett.* **B648** (2007) 201–206, [arXiv:hep-ph/0607045 \[hep-ph\]](#).
 - [3] E. Ma, “Neutrino Mass Matrix from Delta(27) Symmetry,” *Mod. Phys. Lett.* **A21** (2006) 1917–1921, [arXiv:hep-ph/0607056 \[hep-ph\]](#).
 - [4] E. Ma, “Near tribimaximal neutrino mixing with Delta(27) symmetry,” *Phys. Lett.* **B660** (2008) 505–507, [arXiv:0709.0507 \[hep-ph\]](#).
 - [5] F. Bazzocchi and I. de Medeiros Varzielas, “Tri-bi-maximal mixing in viable family symmetry unified model with extended seesaw,” *Phys. Rev.* **D79** (2009) 093001, [arXiv:0902.3250 \[hep-ph\]](#).
 - [6] I. de Medeiros Varzielas and D. Emmanuel-Costa, “Geometrical CP Violation,” *Phys. Rev.* **D84** (2011) 117901, [arXiv:1106.5477 \[hep-ph\]](#).
 - [7] I. de Medeiros Varzielas, D. Emmanuel-Costa, and P. Leser, “Geometrical CP Violation from Non-Renormalisable Scalar Potentials,” *Phys. Lett.* **B716** (2012) 193–196, [arXiv:1204.3633 \[hep-ph\]](#).
 - [8] G. Bhattacharyya, I. de Medeiros Varzielas, and P. Leser, “A common origin of fermion mixing and geometrical CP violation, and its test through Higgs physics at the LHC,” *Phys. Rev. Lett.* **109** (2012) 241603, [arXiv:1210.0545 \[hep-ph\]](#).
 - [9] P. M. Ferreira, W. Grimus, L. Lavoura, and P. O. Ludl, “Maximal CP Violation in Lepton Mixing from a Model with Delta(27) flavour Symmetry,” *JHEP* **09** (2012) 128, [arXiv:1206.7072 \[hep-ph\]](#).
 - [10] E. Ma, “Neutrino Mixing and Geometric CP Violation with Delta(27) Symmetry,” *Phys. Lett.* **B723** (2013) 161–163, [arXiv:1304.1603 \[hep-ph\]](#).
 - [11] C. C. Nishi, “Generalized CP symmetries in $\Delta(27)$ flavor models,” *Phys. Rev.* **D88** no. 3, (2013) 033010, [arXiv:1306.0877 \[hep-ph\]](#).
 - [12] I. de Medeiros Varzielas and D. Pidt, “Towards realistic models of quark masses with geometrical CP violation,” *J. Phys.* **G41** (2014) 025004, [arXiv:1307.0711 \[hep-ph\]](#).
 - [13] A. Aranda, C. Bonilla, S. Morisi, E. Peinado, and J. W. F. Valle, “Dirac neutrinos from flavor symmetry,” *Phys. Rev.* **D89** no. 3, (2014) 033001, [arXiv:1307.3553 \[hep-ph\]](#).
 - [14] I. de Medeiros Varzielas and D. Pidt, “Geometrical CP violation with a complete fermion sector,” *JHEP* **11** (2013) 206, [arXiv:1307.6545 \[hep-ph\]](#).
 - [15] P. F. Harrison, R. Krishnan, and W. G. Scott, “Deviations from tribimaximal neutrino mixing using a model with $\Delta(27)$ symmetry,” *Int. J. Mod. Phys.* **A29** no. 18, (2014) 1450095, [arXiv:1406.2025 \[hep-ph\]](#).
 - [16] E. Ma and A. Natale, “Scotogenic Z_2 or $U(1)_D$ Model of Neutrino Mass with $\Delta(27)$ Symmetry,” *Phys. Lett.* **B734** (2014) 403–405, [arXiv:1403.6772 \[hep-ph\]](#).

- [17] M. Abbas and S. Khalil, “Fermion masses and mixing in $\Delta(27)$ flavour model,” *Phys. Rev.* **D91** no. 5, (2015) 053003, [arXiv:1406.6716 \[hep-ph\]](#).
- [18] M. Abbas, S. Khalil, A. Rashed, and A. Sil, “Neutrino masses and deviation from tribimaximal mixing in $\Delta(27)$ model with inverse seesaw mechanism,” *Phys. Rev.* **D93** no. 1, (2016) 013018, [arXiv:1508.03727 \[hep-ph\]](#).
- [19] I. de Medeiros Varzielas, “ $\Delta(27)$ family symmetry and neutrino mixing,” *JHEP* **08** (2015) 157, [arXiv:1507.00338 \[hep-ph\]](#).
- [20] F. Björkeröth, F. J. de Anda, I. de Medeiros Varzielas, and S. F. King, “Towards a complete $\Delta(27) \times SO(10)$ SUSY GUT,” *Phys. Rev.* **D94** no. 1, (2016) 016006, [arXiv:1512.00850 \[hep-ph\]](#).
- [21] P. Chen, G.-J. Ding, A. D. Rojas, C. A. Vaquera-Araujo, and J. W. F. Valle, “Warped flavor symmetry predictions for neutrino physics,” *JHEP* **01** (2016) 007, [arXiv:1509.06683 \[hep-ph\]](#).
- [22] V. V. Vien, A. E. Cárcamo Hernández, and H. N. Long, “The $\Delta(27)$ flavor 3-3-1 model with neutral leptons,” *Nucl. Phys.* **B913** (2016) 792–814, [arXiv:1601.03300 \[hep-ph\]](#).
- [23] A. E. Cárcamo Hernández, H. N. Long, and V. V. Vien, “A 3-3-1 model with right-handed neutrinos based on the $\Delta(27)$ family symmetry,” *Eur. Phys. J.* **C76** no. 5, (2016) 242, [arXiv:1601.05062 \[hep-ph\]](#).
- [24] F. Björkeröth, F. J. de Anda, I. de Medeiros Varzielas, and S. F. King, “Leptogenesis in a $\Delta(27) \times SO(10)$ SUSY GUT,” *JHEP* **01** (2017) 077, [arXiv:1609.05837 \[hep-ph\]](#).
- [25] A. E. Cárcamo Hernández, S. Kovalenko, J. W. F. Valle, and C. A. Vaquera-Araujo, “Predictive Pati-Salam theory of fermion masses and mixing,” *JHEP* **07** (2017) 118, [arXiv:1705.06320 \[hep-ph\]](#).
- [26] I. de Medeiros Varzielas, G. G. Ross, and J. Talbert, “A Unified Model of Quarks and Leptons with a Universal Texture Zero,” *JHEP* **03** (2018) 007, [arXiv:1710.01741 \[hep-ph\]](#).
- [27] N. Bernal, A. E. Cárcamo Hernández, I. de Medeiros Varzielas, and S. Kovalenko, “Fermion masses and mixings and dark matter constraints in a model with radiative seesaw mechanism,” *JHEP* **05** (2018) 053, [arXiv:1712.02792 \[hep-ph\]](#).
- [28] A. E. Cárcamo Hernández, H. N. Long, and V. V. Vien, “The first $\Delta(27)$ flavor 3-3-1 model with low scale seesaw mechanism,” *Eur. Phys. J.* **C78** no. 10, (2018) 804, [arXiv:1803.01636 \[hep-ph\]](#).
- [29] I. De Medeiros Varzielas, M. L. López-Ibáñez, A. Melis, and O. Vives, “Controlled flavor violation in the MSSM from a unified $\Delta(27)$ flavor symmetry,” *JHEP* **09** (2018) 047, [arXiv:1807.00860 \[hep-ph\]](#).
- [30] A. E. Cárcamo Hernández, S. Kovalenko, J. W. F. Valle, and C. A. Vaquera-Araujo, “Neutrino predictions from a left-right symmetric flavored extension of the standard model,” *JHEP* **02** (2019) 065, [arXiv:1811.03018 \[hep-ph\]](#).
- [31] A. E. Cárcamo Hernández, J. C. Gómez-Izquierdo, S. Kovalenko, and M. Mondragón, “ $\Delta(27)$ flavor singlet-triplet Higgs model for fermion masses and mixings,” *Nucl. Phys.* **B946** (2019) 114688, [arXiv:1810.01764 \[hep-ph\]](#).
- [32] E. Ma, “Scotogenic cobimaximal Dirac neutrino mixing from $\Delta(27)$ and $U(1)_X$,” *Eur. Phys. J.* **C79** no. 11, (2019) 903, [arXiv:1905.01535 \[hep-ph\]](#).
- [33] F. Björkeröth, I. de Medeiros Varzielas, M. L. López-Ibáñez, A. Melis, and O. Vives, “Leptogenesis in $\Delta(27)$ with a Universal Texture Zero,” *JHEP* **09** (2019) 050, [arXiv:1904.10545 \[hep-ph\]](#).
- [34] A. E. Cárcamo Hernández and I. de Medeiros Varzielas, “ $\Delta(27)$ framework for cobimaximal neutrino mixing models,” *Phys. Lett.* **B806** (2020) 135491, [arXiv:2003.01134 \[hep-ph\]](#).
- [35] M. A. Díaz, B. Koch, and S. Urrutia-Quiroga, “Constraints to Dark Matter from Inert Higgs Doublet Model,” *Adv. High Energy Phys.* **2016** (2016) 8278375, [arXiv:1511.04429 \[hep-ph\]](#).
- [36] M. Escudero, A. Berlin, D. Hooper, and M.-X. Lin, “Toward (Finally!) Ruling Out Z and Higgs Mediated Dark Matter Models,” *JCAP* **1612** (2016) 029, [arXiv:1609.09079 \[hep-ph\]](#).
- [37] C. Arbeláez, A. E. Cárcamo Hernández, S. Kovalenko, and I. Schmidt, “Radiative Seesaw-type Mechanism of Fermion Masses and Non-trivial Quark Mixing,” *Eur. Phys. J.* **C77** no. 6, (2017) 422, [arXiv:1602.03607 \[hep-ph\]](#).
- [38] C. Garcia-Cely, M. Gustafsson, and A. Ibarra, “Probing the Inert Doublet Dark Matter Model with Cherenkov Telescopes,” *JCAP* **1602** (2016) 043, [arXiv:1512.02801 \[hep-ph\]](#).
- [39] F. Rojas-Abatte, M. L. Mora, J. Urbina, and A. R. Zerwekh, “Inert two-Higgs-doublet model strongly coupled to a non-Abelian vector resonance,” *Phys. Rev.* **D96** no. 9, (2017) 095025, [arXiv:1707.04543 \[hep-ph\]](#).
- [40] B. Dutta, G. Palacio, J. D. Ruiz-Alvarez, and D. Restrepo, “Vector Boson Fusion in the Inert Doublet Model,” *Phys. Rev.* **D97** no. 5, (2018) 055045, [arXiv:1709.09796 \[hep-ph\]](#).
- [41] T. Nomura and H. Okada, “A radiative seesaw model with higher order terms under an alternative $U(1)_{B-L}$,” *Phys. Lett.* **B781** (2018) 561–567, [arXiv:1711.05115 \[hep-ph\]](#).
- [42] A. E. Cárcamo Hernández and H. N. Long, “A highly predictive A_4 flavour 3-3-1 model with radiative inverse seesaw mechanism,” *J. Phys.* **G45** no. 4, (2018) 045001, [arXiv:1705.05246 \[hep-ph\]](#).
- [43] A. E. Cárcamo Hernández, S. Kovalenko, H. N. Long, and I. Schmidt, “A variant of 3-3-1 model for the generation of the

- SM fermion mass and mixing pattern,” *JHEP* **07** (2018) 144, [arXiv:1705.09169 \[hep-ph\]](#).
- [44] C. Gao, M. A. Luty, and N. A. Neill, “Almost Inert Higgs Bosons at the LHC,” *JHEP* **09** (2019) 043, [arXiv:1812.08179 \[hep-ph\]](#).
- [45] H. N. Long, N. V. Hop, L. T. Hue, N. H. Thao, and A. E. Cárcamo Hernández, “Some phenomenological aspects of the 3-3-1 model with the Cárcamo-Kovalenko-Schmidt mechanism,” *Phys. Rev.* **D100** no. 1, (2019) 015004, [arXiv:1810.00605 \[hep-ph\]](#).
- [46] A. E. Cárcamo Hernández, S. Kovalenko, R. Pasechnik, and I. Schmidt, “Sequentially loop-generated quark and lepton mass hierarchies in an extended Inert Higgs Doublet model,” *JHEP* **06** (2019) 056, [arXiv:1901.02764 \[hep-ph\]](#).
- [47] S. Bhattacharya, P. Ghosh, A. K. Saha, and A. Sil, “Two component dark matter with inert Higgs doublet: neutrino mass, high scale validity and collider searches,” *JHEP* **03** (2020) 090, [arXiv:1905.12583 \[hep-ph\]](#).
- [48] Z.-L. Han and W. Wang, “Predictive Scotogenic Model with Flavor Dependent Symmetry,” *Eur. Phys. J.* **C79** no. 6, (2019) 522, [arXiv:1901.07798 \[hep-ph\]](#).
- [49] A. E. Cárcamo Hernández, S. Kovalenko, R. Pasechnik, and I. Schmidt, “Phenomenology of an extended IDM with loop-generated fermion mass hierarchies,” *Eur. Phys. J.* **C79** no. 7, (2019) 610, [arXiv:1901.09552 \[hep-ph\]](#).
- [50] A. E. Cárcamo Hernández, D. T. Huong, and H. N. Long, “Minimal model for the fermion flavor structure, mass hierarchy, dark matter, leptogenesis, and the electron and muon anomalous magnetic moments,” *Phys. Rev.* **D102** no. 5, (2020) 055002, [arXiv:1910.12877 \[hep-ph\]](#).
- [51] A. E. Cárcamo Hernández, J. W. F. Valle, and C. A. Vaquera-Araujo, “Simple theory for scotogenic dark matter with residual matter-parity,” *Phys. Lett.* **B809** (2020) 135757, [arXiv:2006.06009 \[hep-ph\]](#).
- [52] R. Gonzalez Felipe, H. Serodio, and J. P. Silva, “Neutrino masses and mixing in A4 models with three Higgs doublets,” *Phys. Rev.* **D88** no. 1, (2013) 015015, [arXiv:1304.3468 \[hep-ph\]](#).
- [53] K. Fukuura, T. Miura, E. Takasugi, and M. Yoshimura, “Maximal CP violation, large mixings of neutrinos and democratic type neutrino mass matrix,” *Phys. Rev.* **D61** (2000) 073002, [arXiv:hep-ph/9909415 \[hep-ph\]](#).
- [54] T. Miura, E. Takasugi, and M. Yoshimura, “Large CP violation, large mixings of neutrinos and the Z(3) symmetry,” *Phys. Rev.* **D63** (2001) 013001, [arXiv:hep-ph/0003139 \[hep-ph\]](#).
- [55] E. Ma, “The All purpose neutrino mass matrix,” *Phys. Rev.* **D66** (2002) 117301, [arXiv:hep-ph/0207352 \[hep-ph\]](#).
- [56] E. Ma, “Neutrino mixing: A_4 variations,” *Phys. Lett.* **B752** (2016) 198–200, [arXiv:1510.02501 \[hep-ph\]](#).
- [57] E. Ma, “Soft $A_4 \rightarrow Z_3$ symmetry breaking and cobimaximal neutrino mixing,” *Phys. Lett.* **B755** (2016) 348–350, [arXiv:1601.00138 \[hep-ph\]](#).
- [58] A. Damanik, “Neutrino masses from a cobimaximal neutrino mixing matrix,” [arXiv:1702.03214 \[physics.gen-ph\]](#).
- [59] E. Ma and G. Rajasekaran, “Cobimaximal neutrino mixing from A_4 and its possible deviation,” *EPL* **119** no. 3, (2017) 31001, [arXiv:1708.02208 \[hep-ph\]](#).
- [60] E. Ma, “Cobimaximal neutrino mixing from $S_3 \times Z_2$,” *Phys. Lett.* **B777** (2018) 332–334, [arXiv:1707.03352 \[hep-ph\]](#).
- [61] W. Grimus and L. Lavoura, “Cobimaximal lepton mixing from soft symmetry breaking,” *Phys. Lett.* **B774** (2017) 325–331, [arXiv:1708.09809 \[hep-ph\]](#).
- [62] E. Ma, “Two-loop Z_4 Dirac neutrino masses and mixing, with self-interacting dark matter,” *Nucl. Phys.* **B946** (2019) 114725, [arXiv:1907.04665 \[hep-ph\]](#).
- [63] D. Das, M. L. López-Ibáñez, M. J. Pérez, and O. Vives, “Effective theories of flavor and the nonuniversal MSSM,” *Phys. Rev. D* **95** no. 3, (2017) 035001, [arXiv:1607.06827 \[hep-ph\]](#).
- [64] M. L. López-Ibáñez, A. Melis, M. J. Pérez, and O. Vives, “Slepton non-universality in the flavor-effective MSSM,” *JHEP* **11** (2017) 162, [arXiv:1710.02593 \[hep-ph\]](#). [Erratum: *JHEP* 04, 015 (2018)].
- [65] M. L. López-Ibáñez, A. Melis, D. Meloni, and O. Vives, “Lepton flavor violation and neutrino masses from A_5 and CP in the non-universal MSSM,” *JHEP* **06** (2019) 047, [arXiv:1901.04526 \[hep-ph\]](#).
- [66] M. E. Cabrera, J. A. Casas, A. Delgado, and S. Robles, “2HDM singlet portal to dark matter,” [arXiv:2011.09101 \[hep-ph\]](#).
- [67] I. de Medeiros Varzielas, S. F. King, C. Luhn, and T. Neder, “CP-odd invariants for multi-Higgs models: applications with discrete symmetry,” *Phys. Rev.* **D94** no. 5, (2016) 056007, [arXiv:1603.06942 \[hep-ph\]](#).
- [68] I. de Medeiros Varzielas, S. F. King, C. Luhn, and T. Neder, “Minima of multi-Higgs potentials with triplets of $\Delta(3n^2)$ and $\Delta(6n^2)$,” *Phys. Lett.* **B775** (2017) 303–310, [arXiv:1704.06322 \[hep-ph\]](#).
- [69] F. Staub, “SARAH,” [arXiv:0806.0538 \[hep-ph\]](#).
- [70] F. Staub, “SARAH 4 : A tool for (not only SUSY) model builders,” *Comput. Phys. Commun.* **185** (2014) 1773–1790, [arXiv:1309.7223 \[hep-ph\]](#).
- [71] W. Porod, F. Staub, and A. Vicente, “A Flavor Kit for BSM models,” *Eur. Phys. J.* **C74** no. 8, (2014) 2992,

- [arXiv:1405.1434 \[hep-ph\]](#).
- [72] M. Goodsell, K. Nickel, and F. Staub, “Generic two-loop Higgs mass calculation from a diagrammatic approach,” *Eur. Phys. J. C* **75** no. 6, (2015) 290, [arXiv:1503.03098 \[hep-ph\]](#).
 - [73] F. Staub, “Exploring new models in all detail with SARAH,” *Adv. High Energy Phys.* **2015** (2015) 840780, [arXiv:1503.04200 \[hep-ph\]](#).
 - [74] M. D. Goodsell and F. Staub, “Unitarity constraints on general scalar couplings with SARAH,” *Eur. Phys. J. C* **78** no. 8, (2018) 649, [arXiv:1805.07306 \[hep-ph\]](#).
 - [75] W. Porod, “SPHeno, a program for calculating supersymmetric spectra, SUSY particle decays and SUSY particle production at e^+e^- colliders,” *Comput. Phys. Commun.* **153** (2003) 275–315, [arXiv:hep-ph/0301101 \[hep-ph\]](#).
 - [76] W. Porod and F. Staub, “SPHeno 3.1: Extensions including flavour, CP-phases and models beyond the MSSM,” *Comput. Phys. Commun.* **183** (2012) 2458–2469, [arXiv:1104.1573 \[hep-ph\]](#).
 - [77] Z.-z. Xing, “Flavor structures of charged fermions and massive neutrinos,” *Phys. Rept.* **854** (2020) 1–147, [arXiv:1909.09610 \[hep-ph\]](#).
 - [78] **Particle Data Group** Collaboration, P. A. Zyla *et al.*, “Review of Particle Physics,” *PTEP* **2020** no. 8, (2020) 083C01.
 - [79] P. F. de Salas, D. V. Forero, S. Gariazzo, P. Martínez-Miravé, O. Mena, C. A. Ternes, M. Tórtola, and J. W. F. Valle, “2020 Global reassessment of the neutrino oscillation picture,” [arXiv:2006.11237 \[hep-ph\]](#).
 - [80] I. Esteban, M. C. Gonzalez-Garcia, M. Maltoni, T. Schwetz, and A. Zhou, “The fate of hints: updated global analysis of three-flavor neutrino oscillations,” *JHEP* **09** (2020) 178, [arXiv:2007.14792 \[hep-ph\]](#).
 - [81] **CUPID** Collaboration, E. Armengaud *et al.*, “A new limit for neutrinoless double-beta decay of ^{100}Mo from the CUPID-Mo experiment,” [arXiv:2011.13243 \[nucl-ex\]](#).
 - [82] **nEXO** Collaboration, J. B. Albert *et al.*, “Sensitivity and Discovery Potential of nEXO to Neutrinoless Double Beta Decay,” *Phys. Rev. C* **97** no. 6, (2018) 065503, [arXiv:1710.05075 \[nucl-ex\]](#).
 - [83] A. S. Barabash, “Possibilities of future double beta decay experiments to investigate inverted and normal ordering region of neutrino mass,” *Front. in Phys.* **6** (2019) 160, [arXiv:1901.11342 \[nucl-ex\]](#).
 - [84] **SINDRUM II** Collaboration, W. H. Bertl *et al.*, “A Search for muon to electron conversion in muonic gold,” *Eur. Phys. J. C* **47** (2006) 337–346.
 - [85] **Mu2e** Collaboration, R. Bernstein, “The Mu2e Experiment,” *Front. in Phys.* **7** (2019) 1, [arXiv:1901.11099 \[physics.ins-det\]](#).
 - [86] **COMET** Collaboration, Y. Kuno, “A search for muon-to-electron conversion at J-PARC: The COMET experiment,” *PTEP* **2013** (2013) 022C01.
 - [87] R. Barlow, “The PRISM/PRIME project,” *Nucl. Phys. B Proc. Suppl.* **218** (2011) 44–49.
 - [88] F. F. Deppisch, P. S. Bhupal Dev, and A. Pilaftsis, “Neutrinos and Collider Physics,” *New J. Phys.* **17** no. 7, (2015) 075019, [arXiv:1502.06541 \[hep-ph\]](#).
 - [89] H. Ishimori, T. Kobayashi, H. Ohki, Y. Shimizu, H. Okada, and M. Tanimoto, “Non-Abelian Discrete Symmetries in Particle Physics,” *Prog. Theor. Phys. Suppl.* **183** (2010) 1–163, [arXiv:1003.3552 \[hep-th\]](#).